# X-Ray Powder Diffraction

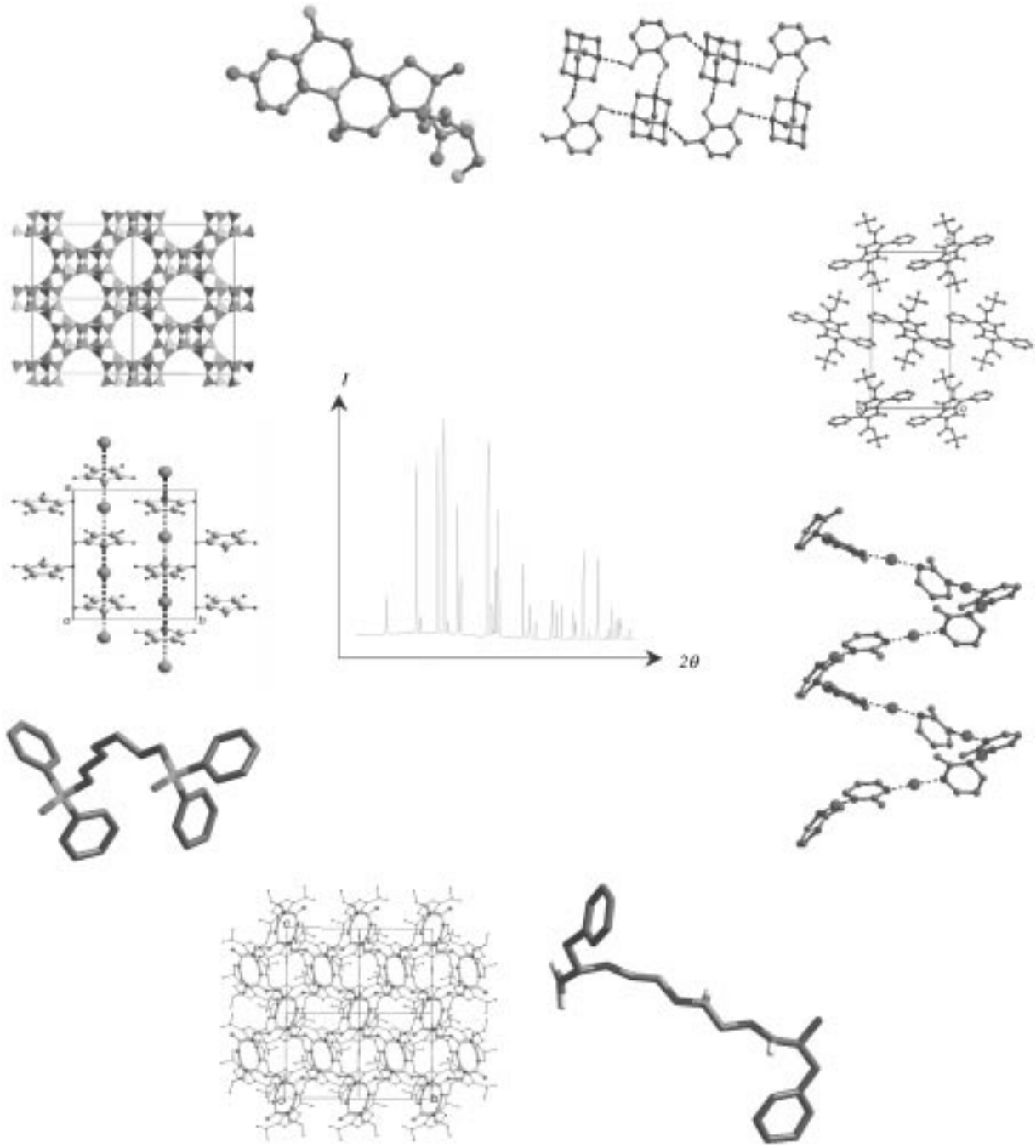


ANGEWANDTE
CHEMIE

# Contemporary Advances in the Use of Powder X-Ray Diffraction for Structure Determination

**Kenneth D. M. Harris,* Maryjane Tremayne, and Benson M. Kariuki**

Many crystalline solids cannot be prepared in the form of single crystals of sufficient size and/or quality for investigation using single-crystal X-ray diffraction techniques, and the opportunity to carry out structure determination using powder diffraction data is therefore essential to understand the structural properties of such materials. Although the refinement stage of the structure determination process can be carried out fairly routinely from powder diffraction data using the Rietveld profile refinement technique, solving crystal structures directly from powder data is associated with several intrinsic difficulties. Nevertheless, substantial progress has been made in recent years in the scope and potential of techniques in this field. This article aims to highlight the types of structural problems for which structure determination may now be tackled directly from powder diffraction data, and contemporary applications across several chemical disciplines are presented. A brief survey of the underlying methodologies is given, with some emphasis on recently developed techniques for carrying out the structure-solution stage of the structure-determination process.

**Keywords:** powder X-ray diffraction · X-ray diffraction · structure elucidation

## 1. Introduction

Single-crystal X-ray diffraction is undoubtedly the most important and powerful technique for elucidation of crystal and molecular structures, and many of the most important scientific advances in the 20th Century emanated from the use of this technique. There is every reason to forecast that the central importance of this technique, both in the physical and biological sciences, will be sustained throughout the 21st Century, particularly by exploiting new opportunities created by advanced synchrotron radiation sources. In emphasizing the power of single-crystal diffraction methods, however, it is important not to overlook the intrinsic requirement that a single crystal of appropriate size and quality must be available for the compound of interest. Clearly this requirement imposes a natural limitation on the types of materials and systems that may be studied. How then do we proceed towards the structural characterization of crystalline solids that do not give single crystals of appropriate size and quality? In this case, powder X-ray diffraction can provide the way forward. Although the lower limits in terms of the size and quality of crystals for which study by single-crystal X-ray diffraction is feasible are continually being extended by developments in instrumentation (e.g. so-called "microcrystal" diffraction facilities) and software for data analysis (e.g. for twinned crystals), there remains a substantial subset of crystalline materials which give rise to good quality powder diffraction data but are not amenable to investigation by single-crystal diffraction techniques. The opportunity to establish a detailed structural understanding of such materials clearly relies on the availability of methods for structure determination from powder diffraction data. Fortunately, the last decades of the 20th Century have seen considerable progress in the scope and potential of techniques in this field, and there is every reason to be confident that this progress will continue in the foreseeable future.

The aim of this article is to highlight, for a general chemical audience, some of the areas in which progress has been made in recent years in the development and application of procedures for structure determination by using powder X-ray diffraction data. The main emphasis is on highlighting, through examples (see Section 3), the types of problems that have been tackled successfully to date, with particular emphasis on those problems that have been made tractable by advances in methodology in the last three or four years. As the literature up to about 1996 has been reviewed in detail elsewhere,[1] this article does not aim to provide a comprehensive coverage of all research in the field up to the present time. Instead, we aim to give a contemporary snapshot of the types of structural problems that are within the scope of

[*] Prof. Dr. K. D. M. Harris, Dr. M. Tremayne, Dr. B. M. Kariuki
School of Chemistry
University of Birmingham
Edgbaston, Birmingham B15 2TT (UK)
Fax: (+44) 121-414-7473
E-mail: K.D.M.Harris@bham.ac.uk

  1433-7851/01/4009-1627 $ 17.50+.50/0 

present methodologies for structure determination from powder diffraction data, placing emphasis on applications involving complete structure determination from powder diffraction data (i.e. examples in which indexing, structure solution, and structure refinement have been carried out directly using the powder diffraction data). We focus in particular on the (generally) more challenging structure-solution stage of the structure-determination process, rather than on structure refinement, although clearly both structure solution and refinement are important components of the complete structure-determination process. However, we note that many important applications of Rietveld refinement from powder diffraction data have made use of known structures (related to the structure of interest), or information from other experimental or computational techniques, to derive an initial structural model for refinement. Such examples do not involve structure solution directly from the powder diffraction data, and are considered to lie outside the province of this article. Section 2 provides a brief overview of techniques used in different stages in the structure-determination process, again with emphasis on contemporary advances in techniques for structure solution, and Section 5 gives a more detailed discussion of these techniques and the procedures for their application. Section 4 discusses some comparisons and contrasts between the use of single-crystal diffraction data and powder diffraction data in structure determination.

The examples highlighted in this article are confined entirely to the use of powder X-ray diffraction data, although we note that, in general, many of the principles and techniques covered here are equally applicable to the case of neutron powder diffraction data. The intrinsic complementarity of X-ray diffraction and neutron diffraction is discussed elsewhere.[1, 2]

## 2. Overview of Methods and Strategy

### 2.1. General Aspects

In the diffraction pattern from a crystalline solid (either for single crystal or powder samples), the positions of the diffraction maxima depend on the periodicity of the structure (i.e. the dimensions of the unit cell), whereas the relative intensities of the diffraction maxima depend on the distribu-

K. D. M. Harris

M. Tremayne

B. M. Kariuki

*Kenneth D. M. Harris was born in Alexandria (Scotland) in 1963, and is a graduate of the University of St Andrews (BSc, 1985) and the University of Cambridge (PhD, 1988), where he carried out research for the PhD degree under the supervision of Professor Sir John Meurig Thomas, FRS. On completion of his PhD, he held positions as Lecturer at the University of St Andrews and then at University College London, before moving in 1995 to his present position as Professor of Structural Chemistry at the University of Birmingham. His current research covers several areas of solid-state chemistry, with particular focus on molecular solids. In addition to studies of fundamental structural, dynamic and chemical properties, his interests in technique development have focused recently on the development and application of new methods for solving structures directly from powder diffraction data. He has been awarded the Meldola (1991), Marlow (1996), and Corday-Morgan (1999) medals of the Royal Society of Chemistry, and the Philips Prize (1997) of the British Crystallographic Association, and has held positions as Visiting Professor in Spain, Taiwan, and Japan.*

*Maryjane Tremayne was born in St Asaph (Wales) in 1969. After obtaining a BSc in chemistry and mathematics at the University of St Andrews, she continued her studies there and gained a PhD in chemistry for research on ab initio structure determination from powder X-ray diffraction data. After spending two years of postdoctoral study with Kenneth Harris at University College London, and a further year at Glasgow University with Chris Gilmore, she was awarded a Royal Society University Research Fellowship in 1997. She has recently taken this Fellowship to the University of Birmingham, where her research continues in the structural behavior of organic solid-state materials and the development of structure determination methods from powder diffraction data.*

*Benson M. Kariuki received a BSc from the University of Nairobi in 1986 and a PhD from the University of Cambridge in 1991, both in chemistry. Postdoctoral research in technique development followed, firstly in microcrystal diffraction and then in structural characterization from crystalline powders. He is currently a research fellow in diffraction at the School of Chemistry, University of Birmingham. His research interests include solid state-chemistry and crystal engineering.*

tion of scattering matter (i.e. the atoms, ions, or molecules) within the repeating unit. Crystal structure determination from diffraction data can be divided into three stages: 1) unit-cell determination ("indexing") and symmetry determination (space-group assignment), 2) structure solution, and 3) structure refinement. Determination of the unit cell requires consideration of the peak positions, whereas space-group assignment, structure solution, and structure refinement also require consideration of the relative intensities of diffraction maxima.

In *structure solution*, the aim is to derive an approximate description of the crystal structure, starting from no knowledge of the actual arrangement of atoms, ions, or molecules in the unit cell. If the approximate structure solution is a sufficiently good representation of the true structure, a good quality structure may then be obtained by refinement of this structural model against the experimental diffraction data in the *structure refinement* stage. For powder diffraction data, refinement of crystal structures can be carried out fairly routinely using the Rietveld profile refinement technique.[3, 4] In general, however, structure solution from powder diffraction data is a significantly greater challenge than structure refinement. A schematic overview of the different stages of structure determination from powder diffraction data is shown in Figure 1.

Although single-crystal and powder diffraction patterns contain the same intrinsic information, in the former this information is distributed in three-dimensional space whereas in the latter the three-dimensional diffraction data are "compressed" into one dimension, which generally leads to considerable overlap of peaks in the powder diffraction pattern.[5] Such peak overlap obscures information on the intensities of individual diffraction maxima, and constitutes the main reason for difficulties in solving crystal structures directly from powder diffraction data. In this Section, we provide an overview of the techniques that are currently available for structure solution from powder diffraction data. These techniques can be subdivided into two categories: "traditional" and "direct-space" approaches.

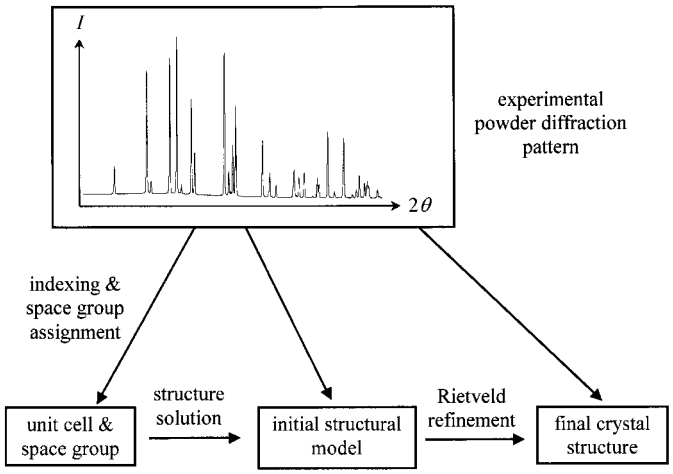


Figure 1. Schematic diagram to illustrate the different stages involved in complete structure determination from powder diffraction data (note that in some cases the situation may be more complex than implied by this diagram).

### 2.2. Traditional Approaches for Structure Solution

In the *traditional approach* for solving crystal structures from powder diffraction data,[1, 6–13] the aim is to extract the intensities $I(hkl)$ of individual reflections directly from the powder diffraction pattern, and then to use these $I(hkl)$ data in the types of structure solution calculation that have been developed for single-crystal diffraction data. These techniques include direct methods and Patterson methods.[14, 15] However, as a consequence of the peak-overlap problem discussed above,[5] it is often difficult to extract unambiguous values of the intensities $I(hkl)$ of the individual diffraction maxima. Unreliable values of the extracted intensities $I(hkl)$ can lead to severe difficulties in subsequent attempts to solve the structure using such "single-crystal-like" techniques. To overcome this problem requires either improved techniques for extracting and utilizing peak intensities or alternative structure-solution strategies that allow the experimental powder diffraction profile to be used directly "as measured" without requiring individual intensities $I(hkl)$ to be extracted. Several important developments in the techniques for extracting and utilizing peak intensities have been reported.[16–25] With regard to details of the traditional techniques for structure solution and their implementation, ref. [1] gives a comprehensive survey of the literature in this field up to 1996, with refs. [12, 13] extending this discussion into subsequent years. Nevertheless, we highlight the following papers which provide details of some of the main programs used in this field: SIRPOW (together with EXTRA in the package EXPO),[26] SIMPEL,[27] XLENS,[28] and ROTSEARCH.[29, 30]

Herein, we focus our discussions of methodology on alternative structure-solution strategies developed in recent years.

### 2.3. Direct-Space Approaches for Structure Solution

In the *direct-space approach*[1, 31, 32] for solving crystal structures from powder diffraction data, trial crystal structures are generated in direct space (independently of the experimental powder diffraction data). The suitability of each trial structure is assessed by direct comparison between the powder diffraction pattern calculated for the trial structure and the experimental powder diffraction pattern. The comparison between the experimental and calculated powder diffraction patterns is quantified using an appropriate figure-of-merit. To date, the majority of direct-space approaches have used the weighted profile $R$ factor $R_{wp}$ (for example, see refs. [33–36]) which is the $R$ factor normally used in Rietveld refinement.[3, 4] As $R_{wp}$ considers the entire digitized powder diffraction profile, rather than the integrated intensities of individual diffraction maxima, peak overlap is implicitly taken into account—the digitized powder diffraction data are used directly "as measured", without further manipulation. The use of $R_{wp}$ to assess the correctness of a structural model clearly requires that the peak-shape and peak-width parameters used to construct the calculated powder diffraction pattern are consistent with those that define the experimental powder diffraction pattern. In practice, this can be readily established

by prior analysis of the peak shapes and peak widths in the experimental powder diffraction pattern (see Section 5.2.2). Other definitions of figure-of-merit such as full profile $\chi^2$[37] or those based on extracted peak intensities[38] have also been used to assess the agreement between calculated and experimental powder diffraction data within the context of direct-space structure solution strategies.

The direct-space strategy for structure solution aims to find the trial crystal structure that has the lowest possible $R$ factor, and the approach is equivalent to exploring a hypersurface $R(\Gamma)$ (Figure 2) to find the global minimum on the hypersurface. Here $\Gamma$ represents the set of variables that defines the structure, as described in more detail below. In principle, any technique for global optimization may be used to locate the lowest point on the $R(\Gamma)$ hypersurface, and success has been achieved using Monte Carlo,[33, 39, 40] simulated annealing,[34–38, 41] grid search,[42–45] and genetic algorithm[46–49] search methods as the basis of direct-space techniques for powder structure solution. Note that the references cited for each technique are intended to be illustrative rather than exhaustive—more citations for each technique are given in Sections 3 and 5.

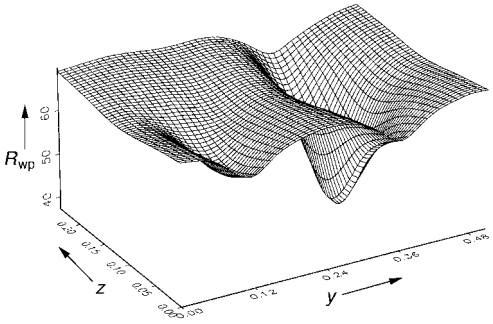


Figure 2. A two-dimensional section through the $R_{wp}$ hypersurface for lithium zirconate ($Li_6Zr_2O_7$). The structural model used to calculate $R_{wp}$ comprised only the zirconium atom (the dominant X-ray scatterer), and thus the structure is specified by three variables—the position ($x$, $y$, $z$) of the zirconium atom. The two-dimensional section $R_{wp}(y,z)$ shown was obtained by fixing the $x$-coordinate of the zirconium atom at the value in the known structure of lithium zirconate. The deep minimum in $R_{wp}$ corresponds to the correct structure solution, but the plot clearly shows the existence of other significant local minima.

As we focus here on structure solution, we assume that the unit cell dimensions ($a$, $b$, $c$, $\alpha$, $\beta$, $\gamma$) and space group are already known from prior analysis of the experimental powder diffraction pattern (see also Section 5.1). We also assume that the contents of the unit cell (for example, the types and number of atoms, ions, or molecules) are known, at least to a sufficiently good approximation, but that the positions and structural arrangement of these constituents within the unit cell are not known. In direct-space techniques, the structure is defined in terms of a "structural fragment" comprising an appropriate collection of atoms within the asymmetric unit, and is defined by a set (denoted $\Gamma$) of variables representing the location of the structural fragment within the unit cell. For a collection of independent atoms, the set $\Gamma$ would comprise the fractional coordinates ($x$, $y$, $z$) for each of these atoms. However, when the structural fragment comprises a molecule of known constitution, it is greatly advantageous to specify the structural fragment in terms of the position and orientation of the molecule as a whole, together with any variables describing unknown aspects of the intramolecular geometry (such as torsion angles), rather than in terms of the fractional coordinates ($x$, $y$, $z$) of each individual atom. Thus, for a molecular fragment, the position may be defined by the fractional coordinates ($x$, $y$, $z$) of the center-of-mass or a predefined pivot atom, the orientation may be defined by rotation angles ($\theta$, $\phi$, $\psi$) around a set of orthogonal axes, and the intramolecular geometry may be specified by a set of $n$ variable torsion angles $\{\tau_1, \tau_2, \ldots, \tau_n\}$. These concepts may be extended to the case of two or more (identical or nonidentical) molecular fragments within the asymmetric unit.

In general, the bond lengths, bond angles, and any known torsion angles (i.e. if the molecular conformation, or aspects of it, are known already) are fixed, and may be taken either from standard values for the type of molecule under study or from the known geometry of a similar molecule (in almost all cases, it is unnecessary to consider bond lengths and bond angles as variables at the structure solution stage). Ideally, the structural fragment should include all atoms with significant scattering power (i.e. all non-hydrogen atoms in the case of powder X-ray diffraction) within the asymmetric unit, but it may sometimes be advantageous to omit certain atoms to restrict the number of variables to be optimized (the omitted atoms may be found later by difference Fourier techniques[1]). Clearly the choice of structural fragment in any given structure solution problem is not unique, although certain choices of structural fragment may have significant advantages over others.

## 2.4. Comparison of Traditional and Direct-Space Approaches

While any comparison of contrasting methodologies must be carried out only with extreme caution, it is nevertheless relevant to make some remarks on the differences between the traditional and direct-space approaches for structure solution from powder diffraction data. The fundamental differences between traditional and direct-space approaches have been outlined above, and here we discuss some practical implications of these differences.

First, we consider aspects of the experimental powder diffraction data itself. As traditional techniques require the intensities of individual reflections extracted directly from the experimental powder diffraction pattern, the reliability of these techniques should be enhanced considerably by using data of higher resolution, as the extent of peak overlap is reduced accordingly. Thus, powder X-ray diffraction data recorded using a synchrotron radiation source[50, 51] should generally be advantageous over data recorded on a conventional laboratory diffractometer (provided there is no severe sample-limited broadening associated with the material under investigation). On the other hand, for direct-space techniques which use a figure-of-merit based on a profile $R$ factor, the important requirement is not high resolution per se, but rather

that the peak profiles are well-defined and accurately described by the peak-shape and peak-width functions used in the structure-solution calculation (as discussed in more detail in Section 5.2). Thus, for direct-space techniques, synchrotron data do not necessarily have intrinsic advantages over laboratory data, particularly if the peak broadening in the synchrotron data is sample-limited rather than instrument-limited.

Second, for structure solution by traditional techniques (as for single-crystal diffraction data), the complexity of the problem generally depends on the number of atoms to be located in the asymmetric unit, whereas for structure solution by direct-space techniques, the main limiting factor is the dimensionality of the hypersurface to be explored (i.e. the number of variables in the set $\Gamma$). Thus, the complexity of a direct-space search procedure (and in general the computational time required to achieve successful structure solution) depends more directly on the number of degrees of freedom in the optimization rather than the number of atoms in the asymmetric unit. As an illustration, direct-space structure solution for a molecule that is large but essentially rigid would generally be more straightforward than structure solution for a molecule that is small but completely flexible (with several torsional degrees of freedom). The greatest challenge in the application of direct-space techniques arises when the number of degrees of freedom required to define the structural fragment is large, and arises either when there is considerable molecular flexibility (i.e. the structural fragment is defined by a significant number of variable torsion angles) and/or when there is more than one independent molecule in the asymmetric unit. Nevertheless, as discussed in Section 3, advances have been made in solving crystal structures that present challenges in each of these categories.

Third, direct-space techniques may be particularly advantageous when the structure contains structural units of well-defined (known) geometry, and for this reason direct-space techniques have found particularly wide application in the case of molecular solids. Similarly, extended framework structures constructed from well-defined building units are also directly amenable to the advantages of direct-space strategies. Traditional techniques, on the other hand, generally do not involve *input* of prior structural knowledge (with some important exceptions, such as fragment based Patterson search techniques[29, 52]), although such knowledge is clearly crucial for the subsequent interpretation of electron-density and Patterson maps. Thus, for problems in which sufficient structural information is already available, there may be certain intrinsic advantages in the use of direct-space techniques, in the sense that prior structural knowledge is used actively *during* the structure solution calculations. Self-evidently, the use of prior structural knowledge in this way is advantageous only if it is confidently known to provide a reliable description of the particular system under investigation.

Fourth, the global-optimization search algorithms embodied within the direct-space techniques for structure solution require, in general, more time to run than typical calculations employing traditional methods for structure solution. However, traditional methods are often less "robust" in the sense that they may often not lead to a satisfactory result, and further computational effort will not, in general, enhance the prospects of successful structure solution further. Furthermore, structure solutions obtained from traditional methods are often incomplete, and may require substantial time to complete the structure (for example using difference Fourier techniques) before final structure refinement can be carried out. As most direct-space approaches (Monte Carlo, simulated annealing, and genetic algorithm methods) are stochastic in nature, it is strongly recommended to run the structure solution calculation several times from different random starting structures—clearly, obtaining the same structure solution from these independent calculations provides strong support that the true global optimum (i.e. the correct structure solution) has been found.

Another important feature of direct-space approaches is that they are based on similar principles to the applications of global-optimization techniques in energy simulations. Thus, as the energy hypersurfaces $E(\Gamma)$ used in energy-based structure prediction calculations and $R$ factor hypersurfaces $R(\Gamma)$ used in direct-space techniques for structure solution are based on the same parameter space $\Gamma$, there are direct opportunities to define hybrid hypersurfaces $G(\Gamma)$ which blend $E(\Gamma)$ and $R(\Gamma)$ together in an appropriate functional form. If the hybrid function $G(\Gamma)$ is defined appropriately, the use of the $G(\Gamma)$ hypersurface in structure solution may have significant advantages over the $R(\Gamma)$ hypersurface. Recently, a strategy has been proposed[53] for combining $R$ factor and energy within the context of a direct-space strategy for structure solution from powder diffraction data, in which the hybrid figure-of-merit uses energy information to guide the calculation towards regions of parameter space corresponding to plausible structures, and the $R$ factor is then used (under the control of a sliding weighting function) as the main criterion for comparing different energetically plausible structures.

## 3. Examples of Structure Determination from Powder Diffraction Data

As discussed in Section 1, many crystalline materials cannot be prepared as crystals of sufficient size and/or quality for single-crystal diffraction studies. Indeed, for many materials of industrial importance, it is actually advantageous to prepare and apply the material in microcrystalline form, for example to increase surface area (e.g. catalysts), to increase dispersibility (e.g. pigments) or to give optimal solubility properties (e.g. pharmaceuticals). Furthermore, most synthetic chemists will be familiar with situations in which, after submitting crystals to the departmental crystallographer, they are told that the crystals are too small, twinned, or simply not good enough to proceed with structure determination. In all these cases, progress towards understanding the structural properties of the materials of interest can be made by exploiting powder diffraction.

Although the majority of the crystal structures that have been determined to date from powder diffraction data are inorganic or framework materials, considerable advances in instrumentation and software for data analysis in recent years

have brought about a rapid evolution in the scope and potential of carrying out structure determination from powder diffraction data for all types of crystalline materials, including molecular solids. As a consequence, the structural properties of materials from many more areas of chemical and materials sciences have now been determined successfully from powder diffraction data.

There are no specific types of materials that can or cannot be studied by powder diffraction, although the optimal technique to be used for structure solution may vary from one class of material to another. The suitability of a material for structure determination depends more on the quality of the powder diffraction data that can be obtained and to some extent the nature of the asymmetric unit (e.g. the number and type of atoms, and how much information is already known about the atomic arrangement (e.g. molecular geometry). However, for successful structure determination, it is highly desirable (although not essential in certain cases, as shown in Section 3.4) that a monophasic powder sample of good crystallinity should be available for the material of interest.

This section highlights some of the structures that have been determined and structural problems that have been tackled from powder diffraction data in recent years, with examples taken from a range of fields and chosen to illustrate the current scope and expanding potential of powder diffraction in structure determination. New techniques developed for powder structure solution in recent years (particularly direct-space techniques) have made greatest impact in the area of molecular crystallography, and we focus on examples from this field. The increasing number and complexity of organic materials for which complete structure determination has been carried out from powder X-ray diffraction data is illustrated in Figure 3.

### 3.1. Studies of Intermolecular Interactions and Crystal Engineering

In crystal engineering, the primary interest centers on understanding the intermolecular aggregation (e.g. hydrogen bonding schemes) in crystals, and subsequently exploiting this understanding in the design of materials with specific desired structures. Although methods are available for the prediction of hydrogen-bonding patterns in specific systems, a detailed description of the hydrogen-bonding pattern in a given system must, in general, be derived from analysis of experimental data. Materials of interest in this field are ideal for direct-space structure solution techniques, particularly when the structures consist of molecular building blocks of well-defined geometry and the main objective is to determine the relative organization of these building blocks within the crystal structure.

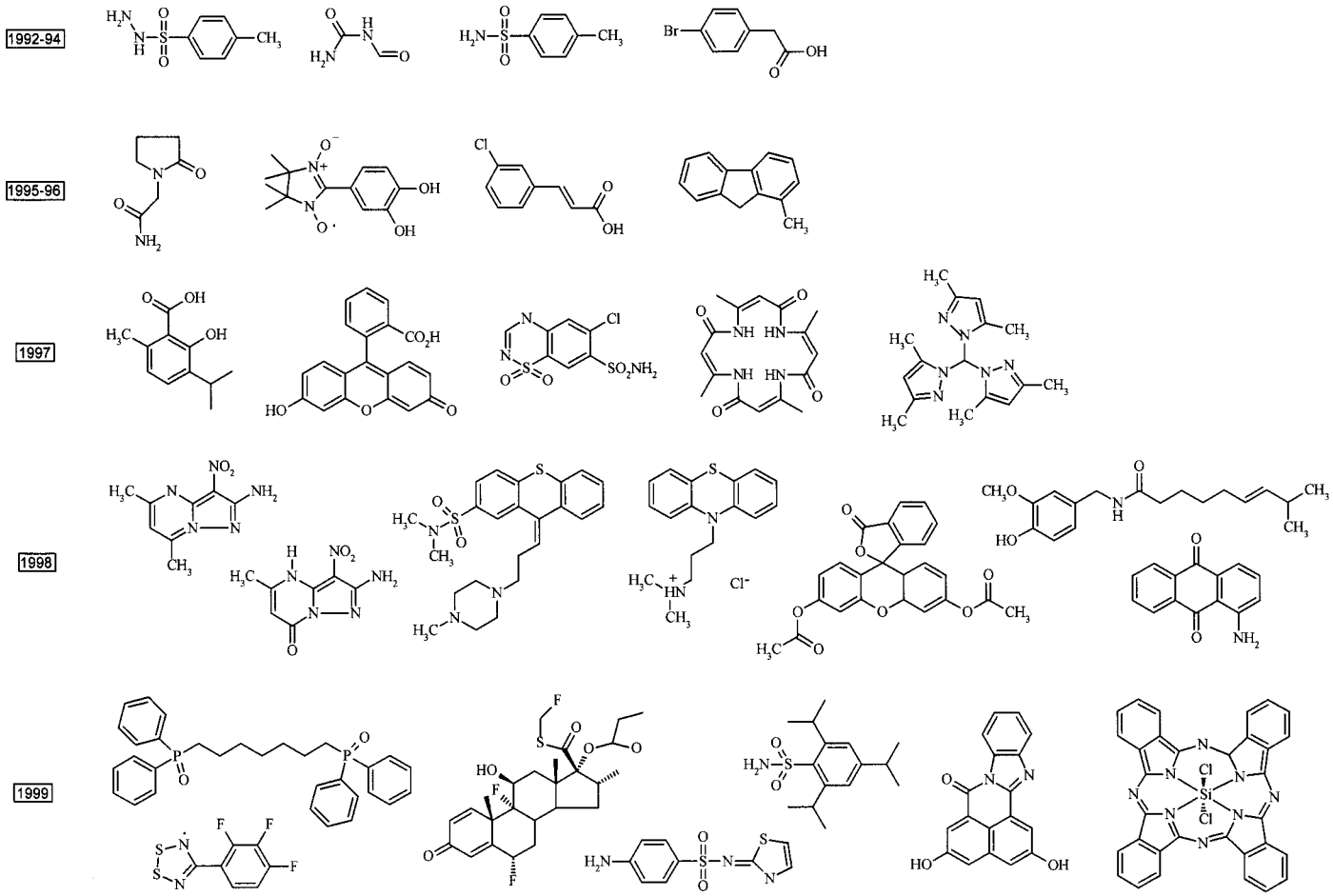


Figure 3. Examples of some of the previously unknown molecular crystal structures for which complete structure determination from powder diffraction data has been carried out in recent years (note that the set of structures shown is representative rather than exhaustive).

Here we highlight the recent structure determination of 2,4,6-triisopropylbenzene sulfonamide $((CH_3)_2CH)_3C_6H_2SO_2NH_2$[54] from powder diffraction data. Crystal-structure solution of this material was initially attempted during a study in which the structures of three related sulfonylamino compounds (4-toluenesulfonamide, benzenesulfonylhydrazide, and 4-toluenesulfonylhydrazide) were solved from powder diffraction data by traditional techniques, and their hydrogen-bonding patterns rationalized.[55] Although the original powder X-ray diffraction data recorded for 2,4,6-triisopropylbenzene sulfonamide at ambient temperature on a laboratory powder X-ray diffractometer were successfully indexed, attempts to solve the structure by traditional techniques were unsuccessful. In the recent study, synchrotron X-ray powder diffraction data were recorded at low temperature, and a relatively straightforward direct-space (Monte Carlo) structure solution calculation was carried out. The structural fragment used in the Monte Carlo calculation comprised the complete molecule (excluding the hydrogen atoms of the methyl groups), with the nitrogen atom entered as an oxygen atom and considered equivalent to the other oxygen atoms in the sulfonylamino group (as no significant discrimination between these atoms would be expected at the structure solution stage). Intramolecular flexibility was introduced in the form of rotation of the isopropyl and sulfonylamino groups relative to the aryl ring (see Figure 4a). Thus, with the molecule also subjected to translation and rotation within the unit cell, each structure considered in the structure solution calculation was defined by ten variables $\{x, y, z, \theta, \phi, \psi, \tau_1, \tau_2, \tau_3, \tau_4\}$. At the structure refinement stage, the nitrogen and oxygen atoms in the sulfonylamino group were readily identified. In the crystal structure, the molecular conformation is found to have the C–H bond of each isopropyl group lying approximately parallel to the plane of the aryl ring, as commonly found in other structures of this type. Elucidation of the crystal structure of this material enables rationalization of the hydrogen-bonding pattern (Figure 4b), which comprises two motifs commonly observed in sulfonamides but not normally occurring together in a given structure. The propagation of these two hydrogen-bonding motifs generates a continuous two-dimensional sheet in which 8-membered and 20-membered rings alternate in a checkerboard pattern.

X-ray powder diffraction has also been used in the structure determination and structural investigation of a hydrogen-bonded molecular solid formed by the 2-(3,4-dihydroxyphenyl)-nitronyl nitroxide radical (see Figure 3—second molecule listed under 1995–96), which is of interest with regard to its magnetic properties.[56] This structure was also solved by an approach that utilizes knowledge of molecular geometry, but based on a full-symmetry Patterson fragment search[29] rather than operating in direct space. The structure was completed using a rigid-body Rietveld refinement and subsequent rationalization confirmed that the molecular aggregation in this material is directed by hydrogen bonding.

The structure determination of $Ph_2P(O)(CH_2)_7P(O)Ph_2$,[57] which is described in detail in Section 3.3, was also part of a wider crystal-engineering study[58] of materials in the family $Ph_2P(O)(CH_2)_nP(O)Ph_2$. The structure solution of the unsolvated crystal form of $Ph_2P(O)(CH_2)_5P(O)Ph_2$ has also been tackled recently from powder diffraction data.[59]

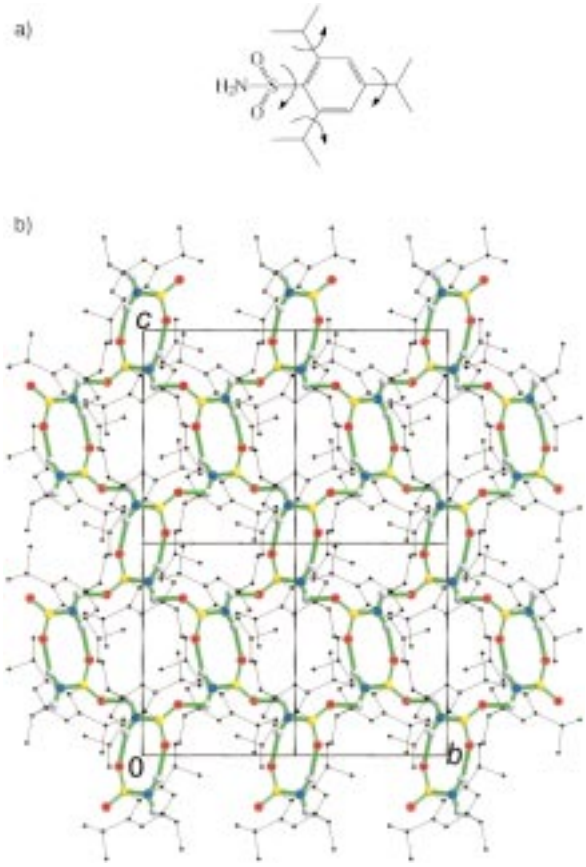


Figure 4. a) Molecular structure of 2,4,6-triisopropylbenzene sulfonamide, with arrows showing the variable torsion angles in the structure-solution calculation. b) View of part of the crystal structure of 2,4,6-triisopropylbenzene sulfonamide showing the 8-membered and 20-membered hydrogen-bonded rings in the (100) plane. Thin black lines represent bonds to carbon, whereas S–N and S=O bonds and N–H···O=S hydrogen bonds are shown by thick green lines.

In the application of direct-space structure solution methods, the presence of more than one type of molecule in the asymmetric unit increases the complexity of the problem, both in terms of the number of degrees of freedom (for two rigid molecules, there are 12 variables in the set $\Gamma$—$\{x_1, y_1, z_1, \theta_1, \phi_1, \psi_1\}$ and $\{x_2, y_2, z_2, \theta_2, \phi_2, \psi_2\}$) and to some extent in terms of $R$ factor discrimination. An example[60] concerns structure determination of the 1:1 cocrystal formed between 1,2,3-trihydroxybenzene and hexamethylenetetramine, using data measured on a conventional laboratory powder X-ray diffractometer. The structure (Figure 5) can be rationalized in terms of puckered hydrogen-bonded molecular ribbons that are linked into a continuous three-dimensional framework by C–H···π(arene) interactions.

Another example concerns the crystal structure of 4-(2,3,4-trifluorophenyl)-1,2,3,5-dithiadiazolyl, which is of interest in the field of molecular magnetic materials. The structure has been determined[61] from powder diffraction data using a direct-space approach based on simulated annealing. In this case, the structural fragment used in the structure-solution calculation comprised two chemically identical, but crystallographically independent, molecules.

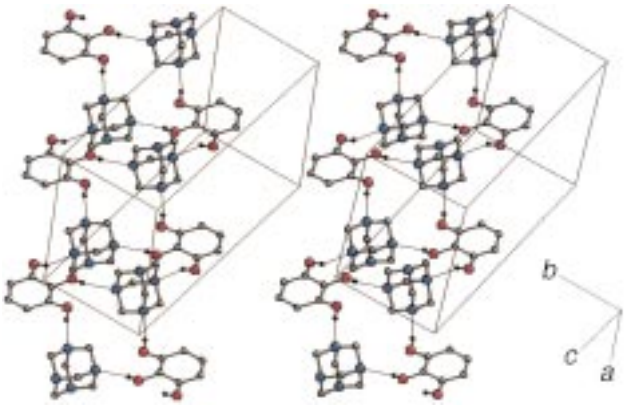


Figure 5. Stereoview of the structure of the cocrystal formed between 1,2,3-trihydroxybenzene and hexamethylenetetramine showing the hydrogen-bonded molecular ribbons running parallel to the *a* axis.

### 3.2. Pharmaceutical Materials

Many drug substances are administered in the form of polycrystalline powders. In such cases, in addition to the intrinsic pharmacological activity of the drug molecule itself, knowledge of the crystal structure is crucial for fully understanding and optimizing the pharmaceutical properties. Relevant aspects in this regard include understanding and controlling solubility, bioavailability, and the conditions for handling and administration. Importantly, a given drug substance administered in different polymorphic forms may lead to very different results. For all these reasons, knowledge of the crystal structures of pharmaceutical materials is of considerable importance, and in many cases powder diffraction provides the only possible route to this information. In addition, the quest to produce and fully characterize all accessible polymorphs[62–64] of a given drug substance has become an area of intense activity within the pharmaceuticals industry in recent years (motivated in part by patenting, registration, and litigation issues), and powder diffraction again has a direct role to play in this regard.

The crystal structures of a number of substances of pharmaceutical interest have been determined from powder diffraction data. Although the first demonstration[65] of ab initio structure solution of a molecular crystal from powder diffraction data by traditional techniques was for the previously known structure of cimetidine (Figure 6) using direct methods, there are only a few other pharmaceutical substances, such as chlorothiazide[66] (a clinically used diuretic compound) and the polymorphic form V of sulfathiazole[67] (an antibacterial drug), for which structure solution using traditional techniques has been reported. The majority of reported structure determinations in this field have employed direct-space techniques for structure solution. Examples include a metastable polymorph of piracetam[68] (a drug used in human therapeutics) studied using the atom – atom potential method and chloroxylenol[69] (an antiseptic) solved using a combination of maximum-entropy and Monte Carlo approaches (see Section 5.3.5). Direct-space approaches have been used to solve the structures of a number of pharmaceutical materials containing conformationally flexible molecules, including ibuprofen[70, 71] (using a genetic algorithm technique) and the tranquilizers promazine hydrochloride and thiothixene[38] (using a simulated annealing technique). The internal degrees of freedom in the structure-solution calculation for thiothixene and the molecular conformation found in the final refined crystal structure are shown in Figure 7. This example illustrates the use of structural knowledge and conformational flexibility in constructing a molecular model for direct-space techniques. While allowing five internal degrees of freedom, the piperazine ring was fixed in a chair conformation and the stereochemistry (*E* versus *Z*) around the C=C bond was fixed in accordance with prior chemical knowledge, thus giving an adequate description of the molecule while keeping the amount of flexibility to the minimum required.

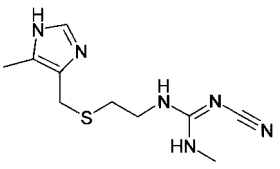

Figure 6. Molecular structure of cimetidine.

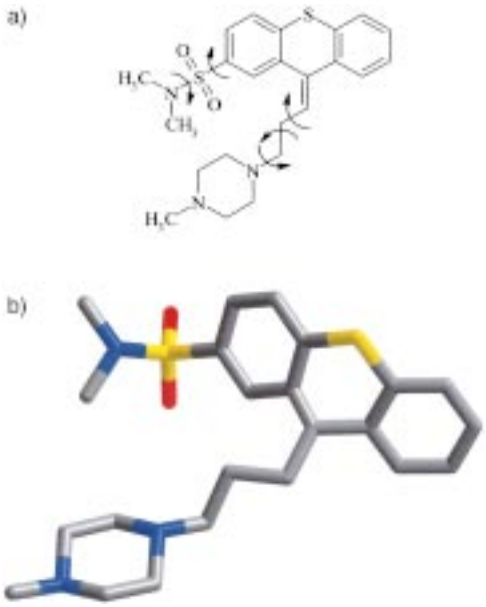


Figure 7. a) Molecular structure of thiothixene, with arrows showing the variable torsion angles in the structure-solution calculation. b) The molecular conformation of thiothixene found in the crystal structure determined from powder diffraction data.

Another example from the pharmaceutical field concerns structure determination of a new polymorph (form 2) of fluticasone propionate,[72] a synthetic anti-inflammatory steroid (Figure 8a). In attempts to produce crystals of fluticasone propionate of controlled size and morphology for pharmaceutical applications, crystallization in a supercritical-fluid medium was carried out, and was found to yield a new polymorph (form 2). As form 2 was obtained only by the supercritical crystallization method, yielding polycrystalline powder samples, structural characterization of form 2 was not possible by single-crystal diffraction. Structure solution from powder diffraction data was carried out using the genetic-algorithm technique, leading (following Rietveld refinement) to the crystal structure shown in Figure 8b.

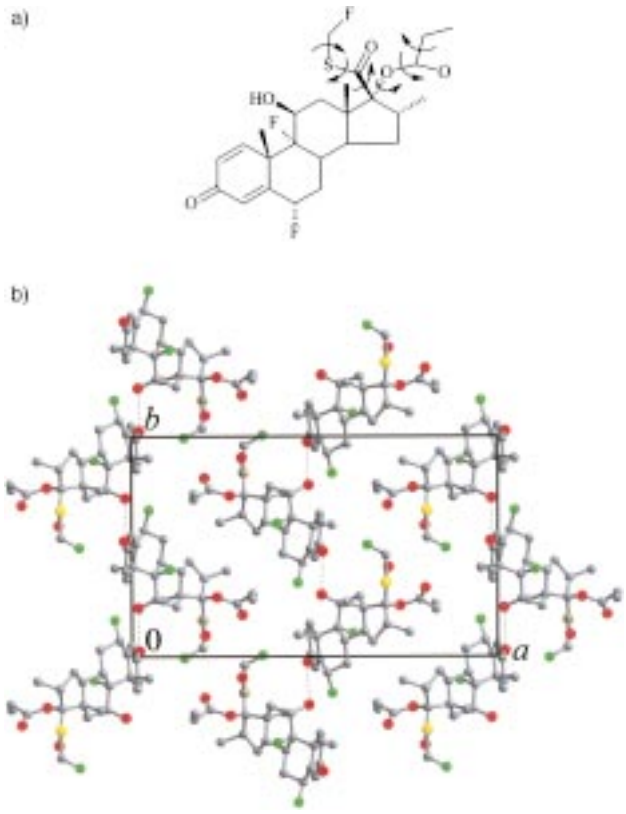


Figure 8. a) Molecular structure of fluticasone propionate, with arrows showing the variable torsion angles in the structure-solution calculation. b) The crystal structure of form 2 of fluticasone propionate (hydrogen atoms not shown) viewed along the *c*-axis. Dashed lines indicate hydrogen-bonding interactions.

### 3.3. Other Organic Materials

X-ray powder diffraction data has been used for crystal structure determination of an increasing number of organic compounds in other fields, and these examples reflect the trends in the structure-solution methods used for molecular materials and the recent growth in the complexity of the problems tackled. As discussed in Section 2.4, the traditional approach for structure solution does not rely on prior knowledge of the geometry of a well-defined structural fragment. However, for "equal-atom" structures (e.g. organic compounds containing no atom heavier than oxygen), the absence of dominant scatterers can make the problems encountered in traditional structure-solution methods particularly severe.[1] To our knowledge, the first previously unknown "equal-atom" organic structure to be solved using direct methods was formylurea.[73] Subsequently, only a few other structures of organic materials have been solved in this way, although the use of high-quality synchrotron X-ray powder diffraction data has been shown to enhance the capabilities of the traditional approach, as illustrated in the structure determination of fluorescein diacetate.[74]

The first material of unknown crystal structure to be solved by a direct-space approach was *p*-$BrC_6H_4CH_2CO_2H$[33] using the Monte Carlo method, followed by other examples using the same method, including 1-methylfluorene[75] and 3-chloro-*trans*-cinnamic acid.[76] The first previously unknown crystal structure to be solved by the genetic-algorithm approach was *ortho*-thymotic acid.[46] Other reported structure determinations from powder diffraction data have included 2,6-naphthalene-dicarboxylic acid and dimethyl 2,6-naphthalenedicarboxylate,[77] as well as materials of potential biological interest including stereoisomeric cyclotetrapeptides derived from 3-aminobutanoic acid,[78] two nitric oxide donors based on pyrazolo[1,5-a]pyrimidine derivatives[79] and an enzyme inhibitor 4-amidinoindanone guanylhydrazone.[80] In other examples, powder X-ray diffraction data have been used in conjunction with computer modeling techniques for structure determination of globular molecules such as norbornane,[81] norbornene,[82] and (*R*,*S*)-camphor.[83]

In all the materials discussed above, the structural fragment is essentially a rigid molecule with at most a few variable torsion angles. However, more complex systems defined by a significant number of torsional degrees of freedom are within the current scope of direct-space structure solution techniques. Thus, direct-space approaches have been used in the complete structure determination of materials such as capsaicin[38] (Figure 9, the "hot" component of chilli peppers), for which ten variable torsion angles were used to define the structural fragment, and heptamethylene-1,7-bis(diphenylphosphane oxide) ($Ph_2P(O)(CH_2)_7P(O)Ph_2$),[57] the structure solution of which is now described in detail.

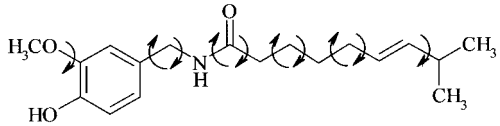


Figure 9. Molecular structure of capsaicin, with arrows showing the variable torsion angles in the structure-solution calculation.

The X-ray powder diffraction pattern of $Ph_2P(O)(CH_2)_7P(O)Ph_2$ was recorded using a conventional laboratory powder X-ray diffractometer, and structure solution was carried out using our genetic-algorithm technique.[49] The structural fragment used in this calculation comprised all non-hydrogen atoms in the molecule, with all bond lengths and bond angles fixed at standard values. A considerable amount of flexibility was required to define the molecular conformation—thus, four torsion angles define the orientations of the phenyl rings (which were themselves constrained to be planar) relative to the remainder of the molecule, and eight torsion angles describe the conformation of the alkyl chain. With the whole molecule also subjected to translation and reorientation within the unit cell, each structure considered in the structure-solution calculation was defined by 18 variables ($\{x, y, z, \theta, \phi, \psi, \tau_1, \tau_2,\ldots\tau_{12}\}$; Figure 10a). In the genetic algorithm structure-solution calculation, the population of crystal structures was allowed to evolve subject to well-defined mating and mutation procedures, leading to the improvement in the quality of the population shown in Figure 11. The best structure in the final generation was used as the starting structural model for Rietveld refinement. In the crystal structure, the molecule adopts a conformation with a *gauche* bond at one position in the alkyl chain (Figure 10b).

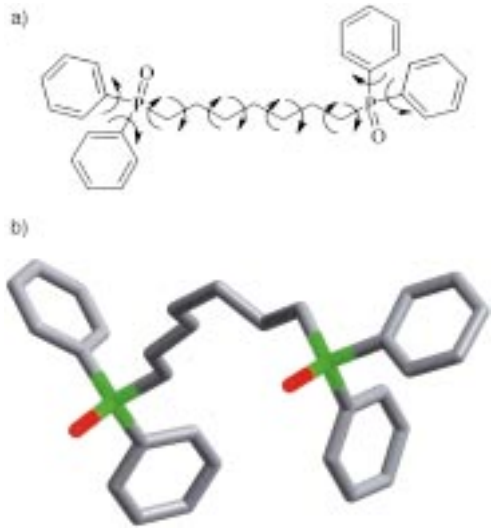


Figure 10. a) Molecular structure of $Ph_2P(O)(CH_2)_7P(O)Ph_2$, with arrows showing the variable torsion angles in the structure solution calculation. b) The molecular conformation of $Ph_2P(O)(CH_2)_7P(O)Ph_2$ found in the crystal structure determined from powder diffraction data.

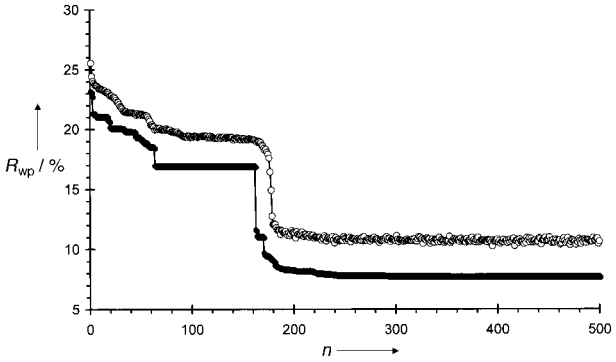


Figure 11. Evolutionary Progress Plot showing the evolution of $R_{wp}$ for the best structure in the population (filled circles) and the average value of $R_{wp}$ for the structures in the population (open circles) as a function of generation number in the genetic algorithm structure solution calculation for $Ph_2P(O)(CH_2)_7P(O)Ph_2$.

It could not have been predicted that this specific molecular conformation would be adopted in the crystal structure, highlighting the importance of allowing conformational flexibility in the structure-solution calculation. The fact that the structure of this material was determined successfully using experimental data collected on a conventional laboratory powder X-ray diffractometer emphasizes that the use of synchrotron data is not essential for powder structure solution, even in the case of complex systems.

Recently, the structure determination of the oligopeptide Phe-Gly-Gly-Phe from powder diffraction data has been reported.[84] The structure was solved using a modified version[85] of the genetic-algorithm technique, based on Lamarckian evolution (discussed in Section 5.3.4). The structure-solution calculation involved 17 structural variables, including 11 variable torsion angles to define the conformation of the Phe-Gly-Gly-Phe molecule (with all peptide groups $R^1$-CO-NH-$R^2$ maintained as planar units with the O-C-N-H dihedral angle fixed at 180°).[86] The crystal structure exhibits a number of interesting features, including hydrogen-bonded ribbons of Phe-Gly-Gly-Phe molecules analogous to an antiparallel $\beta$-sheet, and a double-helix arrangement of hydrogen-bonded chains involving the end groups of the molecules.

In addition to the use of the direct-space techniques highlighted above, variants of the traditional approach in which some knowledge of molecular geometry is incorporated within the structure-solution calculation have also been used. Thus, Patterson-fragment search methods have been used to solve a number of organic crystal structures, including the sublimated form of tris(3,5-dimethylpyrazol-1-yl)methane,[87] L-carvone, and DL-carvone.[30]

### 3.4. Organometallic Complexes

For coordination and organometallic compounds, the presence of a few metal atoms (dominant X-ray scatterers) often simplifies the process of structure solution.[88] Conversely, however, in some cases the presence of a highly dominant scatterer can mask information in the diffraction data concerning the organic component of the material, such that structure solution and structure completion may be more difficult for that part of the structure.

In view of the presence of heavy atoms, it is not surprising that most reported cases of the structure solution of organometallic materials from powder X-ray diffraction data have employed traditional techniques. An example is cyclopentadienyl rubidium,[89] for which the direct methods program SIRPOW[90] was used to locate the rubidium and carbon atoms. In Rietveld refinement, the cyclopentadienyl rings were set up as rigid bodies to stabilize the refinement. An interesting aspect of this study is that the powder sample actually contained two polymorphs of cyclopentadienyl rubidium. Initial attempts to index the powder diffraction pattern failed because of the presence of the two phases, but closer inspection revealed that the peaks could be subdivided into two sets: narrow peaks (with instrument-limited peak widths) and substantially broader peaks. By subdividing the experimental data in this way, both phases were indexed and the structures solved using the approach described above. The structures of the two polymorphs of cyclopentadienyl rubidium determined in this study are shown in Figure 12. The use of synchrotron X-ray powder diffraction data was important in this case, as different types of sample broadening could not be distinguished with the lower instrumental resolution of a conventional laboratory powder X-ray diffractometer.

The crystal structure of silicon phthalocyanine dichloride ($SiPcCl_2$) has been determined recently[91] from powder diffraction data, with structure solution carried out using a direct-space approach based on the Monte Carlo method. Knowledge of this crystal structure has been used, in conjunction with scanning tunneling microscopy data, to understand the structural properties of both low-coverage and high-coverage films of $SiPcCl_2$ deposited on silicon surfaces. In another direct-space application, the structure of the malaria pigment $\beta$-haematin has been determined[92] from powder diffraction data, in this case employing a simulated annealing method for structure solution.

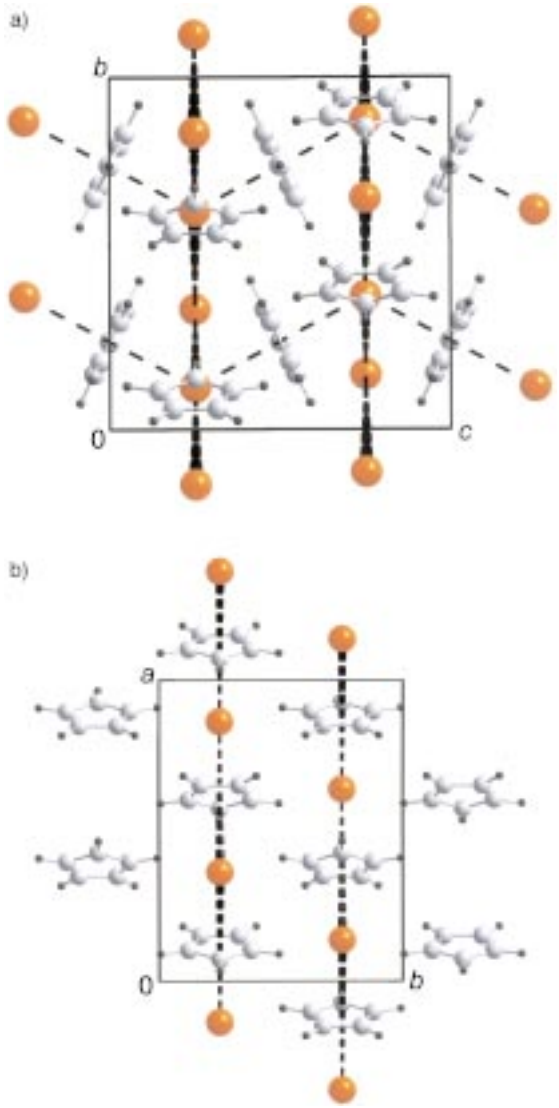


Figure 12. Crystal structures of the two polymorphs of cyclopentadienyl rubidium: a) form I, and b) form II. Dashed lines show distances between near-neighbor rubidium atoms.

### 3.5. Zeolites and Related Materials

Zeolites are microporous solids with a wide-range of commercial applications in catalytic, adsorption, and separation processes.[93–95] As these technologically important properties of zeolites are closely related to their crystal structures, knowledge of the structural properties is central to the design and development of applications of these materials. Unfortunately, however, many synthetic zeolites are available only as powders and cannot be studied using conventional single-crystal diffraction techniques. In such cases, a combination of techniques, such as powder X-ray diffraction, electron microscopy, high-resolution solid state NMR, computer simulation, and model building is commonly used to obtain structural information.[8, 96–98] The crystal structures of a number of zeolitic materials have been solved and refined directly from powder diffraction data, leading to structural knowledge of several new materials and new zeolite structure types.[99] Early examples involving structure solution using traditional approaches included $AlPO_4$-12-TAMU,[100] sigma-2 clathrasil,[101] and anhydrous VPI-5.[102]

A more recent example concerns the large pore, pure silica polymorph ITQ-4.[103] Laboratory X-ray powder diffraction data were used initially to determine the unit cell parameters and high-resolution solid-state $^{29}Si$ NMR showed that there are four different silicon environments in the asymmetric unit. High-resolution synchrotron X-ray powder diffraction data were then used to solve the structure by using the direct-methods program SIRPOW,[90] giving the positions of all the framework atoms. These positions were used as the starting structural model for Rietveld refinement. This structure represents a new zeolite with an exceptionally large pore volume (Figure 13). However, structure solution of zeolitic materials is not often carried out so straightforwardly, and the problems encountered with structure determination in other fields are often exacerbated by the occurrence of disorder, faulting, and other structural defects.

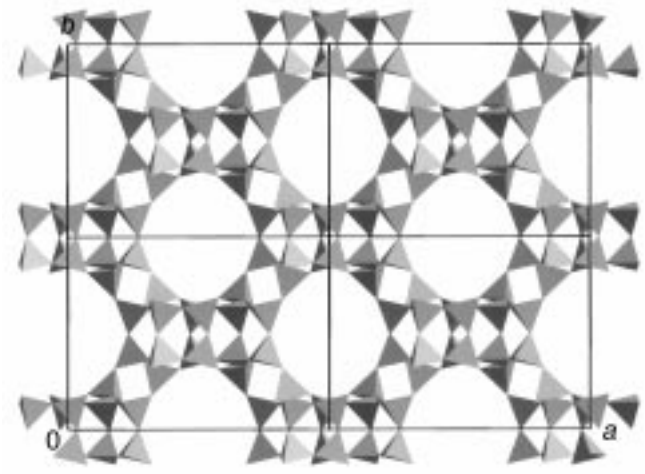


Figure 13. Structure of the large-pore material ITQ-4 (unit cell dimensions are $a = 18.65$, $b = 13.50$, $c = 7.63$ Å, $\beta = 102.0^\circ$).

To overcome difficulties encountered in this field, traditional structure-solution methods are often combined with model building, as used in the structure solution of RUB-10[104] and $AlPO_4$-18.[105] New structure-solution techniques have also been developed by researchers with particular interest in this area. One of the first methods[19] focused on the redistribution of the intensities of overlapping reflections based on the enhancement of a Patterson map. The resulting data were used to solve the structure of SAPO-40, for which previous attempts using equipartitioned data failed. Other methods for structure determination include the use of structure envelopes[106] (see Section 5.3.5), and the FOCUS method,[107–109] which uses powder diffraction data in combination with chemical information in the form of a specialized topology search specific to zeolites.[110] An example of a zeolitic structure (VPI-10) solved using the FOCUS method is shown in Figure 14. Simulated annealing has also been adapted for application to zeolite framework structures,[111, 112] with reliable information on the geometric characteristics of tetrahedral species (Si, Al, etc.) in zeolite frameworks

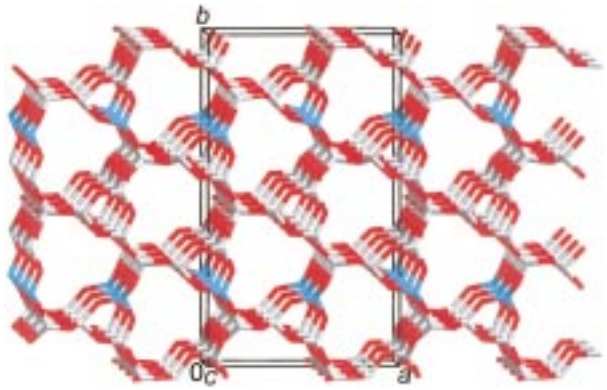


Figure 14. The framework structure of the zincosilicate material VPI-10 solved from powder diffraction data using the FOCUS method. Si: gray; O: red; Zn: blue.

incorporated into the calculation of the figure-of-merit (cost function) used to rank possible framework topologies. This technique has been used to solve the structures of UiO-7[113] and ERS-7.[114] It is clear that the active use of such structural knowledge in the structure determination process enhances the ability to solve more complex zeolitic structures from powder diffraction data.

The structure of the relatively complex material UTD-1[115] has recently been solved using an experimental approach in which several different (but related) powder diffraction patterns are recorded for a textured sample (i.e. a sample exhibiting preferred orientation of the crystallites—see Section 5.5). In this way, data that are more "single-crystal-like" in character can be obtained, and in the case of UTD-1 a standard direct methods program was sufficient to solve the structure from such data.

### 3.6. Polymers

Polymers are of well-proven, wide-ranging technological importance, and it is clearly important to be able to develop a structural understanding of these materials, to rationalize their solid-state properties, and further exploit their applications. Despite the huge molecular size, crystalline polymeric materials are well suited for structure determination as the asymmetric unit often comprises a simple monomer unit. However, good quality polymer crystals are often difficult to obtain, and practitioners in this field often turn to fiber diffraction. When fibers are not available, structural information may be obtained from powder diffraction data.

In the case of organic polymers, poor crystallinity often manifests itself in the broadening of diffraction peaks, which renders traditional techniques for structure solution unsuitable. As a result, examples of successful structure determination (such as poly(*p*-phenylene terephthalate),[116] poly(hydroxybutyrate),[117] and azomethine block-copolymers[118]) have invoked molecular modeling to generate energetically and sterically favorable models, which are then compared and refined against the experimental powder diffraction data.

More traditional methods can be used to study metal-organic polymers which are normally more crystalline than organic polymers.[88] In addition, the presence of a metal atom (i.e. a dominant X-ray scatterer) in the structure can simplify the structure solution process. One research group working in the field of metal diazolates has solved the structures of a number of polymeric complexes directly from powder diffraction data, including those of $[\{Cu(pz)\}_n]$ and $[\{Ag(pz)\}_n]$ (Hpz = pyrazole),[119] $[\{Ag(imz)\}_n]$ (Himz = imidazole),[120] $[\{NiX_2(pydz)\}_n]$ (X = Cl or Br; pydz = pyridazine),[121] and $[\{MX_2(bipy)\}_n]$ (M = Ni or Cu; X = Cl or Br; bipy = 4,4′-bipyridyl).[122] In these cases, structure solution was carried out using the direct-methods program SIRPOW[90] or a grid search technique[123] to locate the dominant X-ray scatterer, and the positions of the remaining ligand atoms were established from simple packing and symmetry considerations. These materials exhibit many interesting structural features. An example concerns $[Cu(pymo)_n]$ (Hpymo = 2-hydroxypyrimidine)[124] was found to be unsuitable for study by single-crystal powder diffraction techniques. Crystal-structure determination from powder data using traditional structure-solution methods revealed that helical polymers and separate hexamers coexist in an ordered fashion in the same crystal phase (Figure 15)—a structural feature that has not previously been reported in any field.

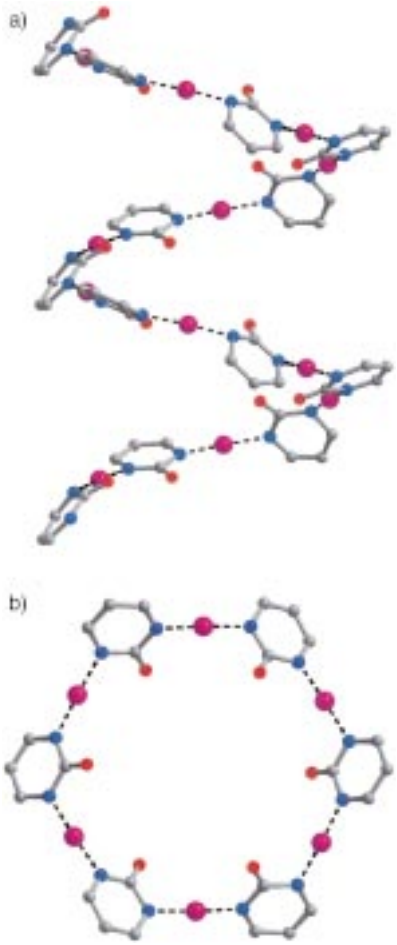


Figure 15. The structural components a) linear polymers and b) cyclic hexamers found in the crystal structure of $[Cu(pymo)_n]$. In the crystal structure, the polymer chains are threaded through the cyclic hexamers, which are stacked on top of each other to generate a channel-like arrangement (not shown).

A family of polymer electrolyte complexes, comprising salts dissolved in poly(ethylene oxide) (PEO), has also been studied by powder diffraction. PEO is a high molecular weight polymer with repeat unit $CH_2CH_2O$. Although the crystal structures of the $(PEO)_3 \cdot NaClO_4$[125] and $(PEO)_3 \cdot LiCF_3SO_3$[126] complexes were determined by Rietveld refinement of a model based on a known structure, no such structural models were available for other complexes, for which structure solution has been carried out directly from powder diffraction data. Thus, the structure of the complex formed between $NH_4SCN$ and PEO (stoichiometry $(PEO)_4 \cdot NH_4SCN$) was solved using traditional direct methods, subsequently enabling the structure refinement of the isostructural systems $(PEO)_4 \cdot KSCN$[127] and $(PEO)_4 \cdot RbSCN$.[128] However, in the case of $(PEO)_3 \cdot LiN(SO_2CF_3)_2$[37] and $(PEO) \cdot NaCF_3SO_3$[129] attempts to refine the structures using a known structure as the starting point were unsuccessful, as was structure solution by traditional approaches. Instead, progress was made using a flexible direct-space approach for structure solution based on a simulated-annealing protocol. Recently,[130] the structure of the $(PEO)_6 \cdot LiAsF_6$ complex has also been determined from powder diffraction data, with structure solution again carried out using a simulated-annealing approach.

### 3.7. Pigments and Dyes

By definition, pigments are colored solid particles that are insoluble in the medium in which the pigment is applied (for example, in paints, plastics, and printing inks), whereas dyes are soluble materials which are used in dissolved or dispersed states in their applications.[131] Clearly the physical properties of pigment materials depend on both molecular and crystal structure. Most pigments can be prepared only as fine powders (poor solubility often prevents growth of good quality single crystals from solution), and for this reason many pigments have eluded crystal-structure determination by single-crystal diffraction techniques. Furthermore, it is important to recognize that for good dispersion and the optimization of other pigment properties, it is generally necessary to prepare and apply real pigment materials as microcrystalline particles. For these reasons, structural characterization of pigment materials falls directly within the scope of powder structure-determination techniques.

Apart from those based on azo chromophores, the majority of organic materials of interest in this field involve heterocyclic chromophores such as phthalocyanines, quinacridones, and anthraquinones, and in general these molecules can be described as rigid structural units of well-defined geometry. Not surprisingly, for most structures in these classes, structure determination from powder diffraction data has focused on direct-space techniques for structure solution, or approaches that combine crystal modeling together with analysis of powder diffraction data. Examples include 6,13-dichlorotriphendioxazine,[132] 1-aminoanthraquinone[133] and the X form of metal-free phthalocyanine.[134]

A crystal-modeling approach has also been used to solve the structure of a perinone pigment—2,5-dihydroxybenzo[*d*,*e*]benzo[4,5]imidazo[2,1-*a*]isoquinolin-7-one[135] (see Figure 3—sixth molecule listed under 1999)—representing the only crystal structure published so far for this class of pigments. Firstly, the powder diffraction pattern was indexed and although a number of possible space groups were consistent with the data, space groups that are rare for organic systems were rejected. The geometry of the molecule used in the structure-solution calculation was constructed from the crystal structures of materials containing similar fragments, and the molecule was assumed to be planar. However, the positions (*exo* or *endo*) of the hydrogen atoms of the hydroxyl groups could not be assigned a priori, and calculations were therefore carried out separately for each of the four conformers (and for each space group). In this regard, it is important to note that energy calculations require the inclusion of hydrogen atoms (whereas structure-solution calculations from powder X-ray diffraction data would not). The crystal structure was "solved" by minimization of intermolecular energy by a steepest-descent algorithm, starting from random crystal-packing arrangements, and the structures obtained were then "screened" by comparison with the experimental X-ray powder diffraction data. A structure giving good agreement between the calculated and experimental powder diffraction patterns was found (although it was not actually the lowest-energy structure found). Refinement of this structure was then carried out by using rigid-body Rietveld analysis.

Other examples from this field have required the introduction of conformational flexibility in the structure-solution calculation, and have been tackled by using direct-space techniques (particularly the Monte Carlo method). Thus, structure determination of the red phase of fluorescein (which finds applications as a yellow dye with intense green fluorescence) from powder diffraction data[39] represented the resolution of a long-standing structural problem.

Another example concerns the structure determination of 1,4-diketo-2,5-di-*tert*-butoxycarbonyl-3,6-diphenyl-pyrrolo[3,4]-pyrrole (DPP-Boc), an important derivative of the commercial red pigment 1,4-diketo-3,6-diphenyl-pyrrolo[3,4-*c*]pyrrole (DPP). An approach developed recently to ensure good dispersion of pigments (such as DPP) in the application medium of interest involves the introduction of the pigment chromophore as a molecule (called a "latent" pigment) which is readily soluble in the application medium. Subsequently, the insoluble pigment particles are generated in situ through an appropriate chemical reaction of the latent pigment. The importance of DPP-Boc lies in its use as a latent pigment,[136] it undergoes a thermal reaction (involving removal of the *tert*-butoxycarbonyl groups) to produce DPP (Figure 16). Recently, routine powder X-ray diffraction studies of this system revealed the existence of a new polymorph ($\beta$ phase) of DPP-Boc[137, 138] in addition to a previously known polymorph ($\alpha$ phase). Here we describe the structure determination of the $\beta$ phase from powder X-ray diffraction data. After determination of the unit cell, density considerations in conjunction with solid-state $^{13}C$ NMR spectroscopic data suggested that the asymmetric unit comprises half the DPP-Boc molecule. The structural fragment used for structure solution comprised all the non-hydrogen atoms in the

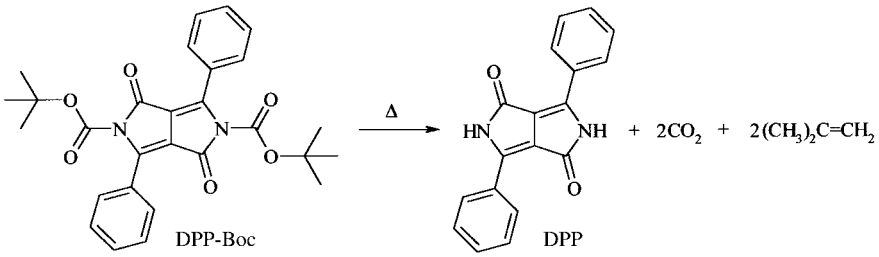


Figure 16. Thermal decomposition of the "latent" pigment DPP-Boc (left) to produce the pigment material DPP (right).

asymmetric unit, and the molecular inversion center was constrained to reside on a crystallographic inversion center (space group $P\bar{1}$). A Monte Carlo calculation was then carried out involving free reorientation of the whole molecule around this pivot point and variation of four torsion angles within the *tert*-butoxycarbonyl group (Figure 17a). The structure with lowest $R_{wp}$ found in the structure solution calculation was then used as the starting model for Rietveld refinement. As for the known $\alpha$ phase of DPP-Boc, the molecules in the $\beta$ phase (Figure 17b) are stacked in columns, although details of the stacking arrangement and the structural relationships between columns differ significantly between the two polymorphs. Clearly powder diffraction played a pivotal role in the study of this material, both in the initial identification of a new polymorph and in the subsequent structure determination.

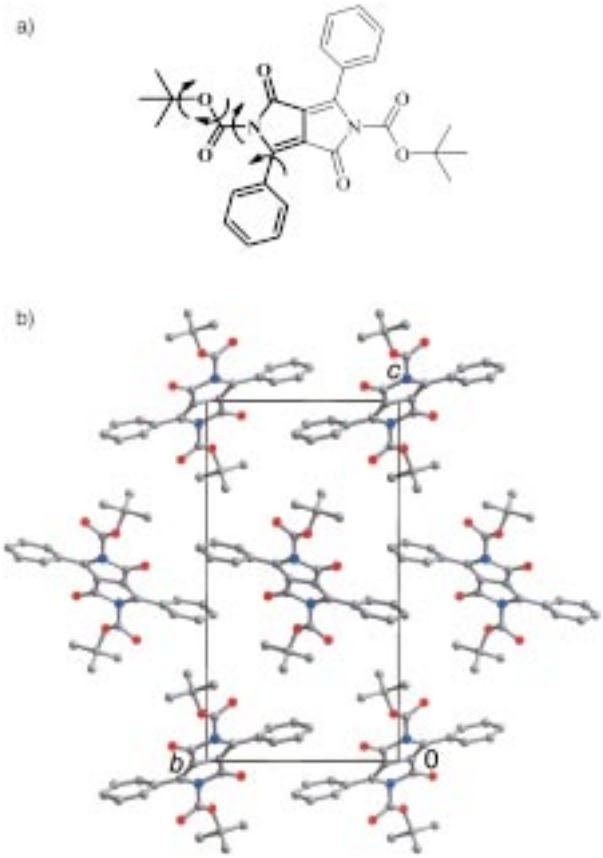


Figure 17. a) Molecular structure of DPP-Boc. The structural fragment used in the structure-solution calculation represents half the molecule (shown as bold), and the arrows indicate the variable torsion angles. b) The crystal structure of the $\beta$ phase of DPP-Boc, determined directly from powder diffraction data.

### 3.8. Solid-State Reactions

It is well known[139–141] that to develop an understanding of the chemical reactivity of solids relies, in the first instance, on knowing the structural properties of the solid and hence establishing the geometric relationships between the molecules, atoms, or ions that are involved in the reaction. Thus, the ability to determine the crystal structures of reactive materials is a crucial prerequisite for understanding the chemical transformations that occur within them, as illustrated by the following examples.

It has been known since the 1850s[142, 143] that solid sodium chloroacetate undergoes a polymerization reaction at sufficiently high temperature to produce polyglycolide and sodium chloride [Eq. (1)]. However, an understanding of this reaction

$$n\,\mathrm{ClCH_2COONa} \longrightarrow n\,\mathrm{NaCl} + [\mathrm{CH_2COO}]_n \qquad (1)$$

and its mechanism was not previously possible, as sodium chloroacetate is microcrystalline and structural information could not be determined using single-crystal X-ray diffraction methods. Recently,[144] the structure of sodium chloroacetate (Figure 18) was determined directly from powder X-ray

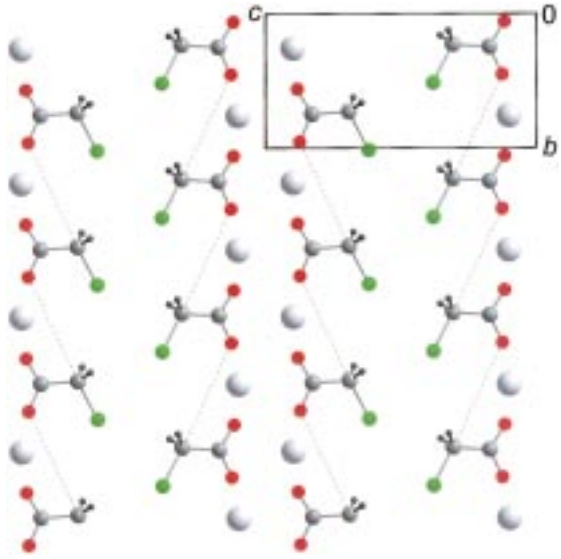


Figure 18. A section of the crystal structure of sodium chloroacetate, with dotted lines indicating the propagation of the polymerization reaction within rows of chloroacetate anions along the *b*-axis.

diffraction data, with the structure solution carried out using the Monte Carlo method. From knowledge of the crystal structure, the polymerization reaction to produce polyglycolide may be rationalized directly on the basis of a topochemical reaction pathway. The crystal structures of various lithium halogenoacetates have also been determined recently from powder diffraction data,[145] and provide a basis for understanding the chemical reactivity of these systems.

## 4. Powder Diffraction Versus Single-Crystal Diffraction

As highlighted throughout this article, one of the main areas of application of powder diffraction is the structural characterization of microcrystalline materials that are unsuitable for investigation by single-crystal diffraction techniques, and as such powder diffraction has considerable importance in several disciplines of solid-state and materials sciences. In addition to this intrinsic difference between powder diffraction and single-crystal diffraction, we now consider some other comparisons and contrasts between these techniques and their applications.

An important application of powder X-ray diffraction across several fields concerns studies of structural changes associated with phase transitions and chemical reactions in solids. From the practical point of view, powder diffraction experiments may be carried out fairly straightforwardly to monitor structural changes in a solid as a function of the variation of external conditions (such as temperature, pressure, or exposure to gaseous atmospheres of varying composition), and in general such in situ studies are more readily carried out by powder diffraction techniques than single-crystal diffraction techniques. Furthermore, it is well known that phase transitions and chemical reactions in single-crystals are often associated with a reduction in crystal quality, for example through twinning, fracturing, or indeed the production of a polycrystalline "daughter" phase from a single-crystal "parent". Clearly there are intrinsic limitations concerning the prospects of monitoring such transformations using single-crystal diffraction, whereas powder diffraction data recorded for the same systems may show little or no deterioration in quality throughout the transformation. In addition, some solid materials of interest (for example, certain clathrate hydrates) may not exist under conditions of ambient temperature and pressure, and for such materials that require synthesis, handling, and characterization under nonambient conditions, powder diffraction generally provides a more straightforward approach for structural characterization than single-crystal diffraction techniques.

In more general terms, crystal twinning and certain other types of defects are a major source of problems in single-crystal diffraction studies (many crystals grow intrinsically in a twinned manner), but may have little or no bearing on the quality of powder diffraction data for the same sample. Thus, the ability to carry out structure determination from powder diffraction data should be unaffected by the occurrence of twinning in the individual crystallites within the powder, provided each individual twin is still sufficiently large that particle-size effects do not give rise to serious line broadening.

In the industrial context, it is important to emphasize that powder diffraction allows materials to be investigated directly under the conditions in which they are used in specific applications, whereas single-crystal diffraction (by virtue of the requirement to prepare and study a single crystal) might not. For example (see also Section 3.2), solid pharmaceutical substances are often administered into the body as compacted powders in the form of tablets. For such materials, it may be important to understand directly (for example, from powder diffraction studies of the tablets) whether they undergo any structural transformation as a consequence of the compaction process. If such transformations do occur, the crystal structure of the actual material administered into the body may be very different from the structure, determined by single-crystal diffraction, of a crystal of the same material grown from solution.

It is relevant to compare the quality of structural information that can be obtained by structure determination using powder versus single-crystal diffraction data. In general, the final structural parameters obtained from powder diffraction data are not as accurate or precise as those that could be determined for the same material from single-crystal diffraction data (assuming that single crystals were available). Thus, although significant differences in bond lengths characteristic of different bond types (for example C=O versus C–OH) may be readily distinguished from powder data, slight deviations from standard bond lengths and bond angles can not, in general, be reliably assessed. For good quality powder diffraction data, the positions of hydrogen atoms can also be determined (for example, see refs [65, 146]), although such atoms are normally placed in calculated positions during structure refinement calculations (rather than explicitly refined). If crystals suitable for single-crystal X-ray diffraction experiments are available, it is clear that this approach remains the technique of choice for accurate and/or routine structure determination. Indeed, it is relevant to note the importance of optimizing crystal-growth strategies to enhance the opportunities of obtaining single crystals of sufficient size and quality for any particular material of interest.[147]

In addition to the use of powder diffraction in allowing structure determination of microcrystalline materials that are unsuitable for investigation by single-crystal diffraction techniques, it has many other important roles in the structural investigation of crystalline materials. Structure determination from powder diffraction data ensures that the bulk solid sample is investigated, in contrast to the potentially unrepresentative procedure of selecting an individual crystal from the sample, as done in single-crystal diffraction. Clearly any individual crystal within a bulk solid sample might not be representative of the bulk material, and could be a different polymorph or an impurity. Thus, when a structure is solved from single-crystal diffraction data, it is good practice to check that this structure is actually representative of the bulk material from which the single crystal was selected, and powder diffraction provides a direct means of checking this fact. Regrettably, this simple step is often ignored. To illustrate the necessity of using powder diffraction in this regard, we consider the case of *p*-formyl-*trans*-cinnamic acid (*p*-FCA),[148] which exists in two polymorphic forms—one polymorph ($\beta$ phase) is photoreactive under UV irradiation, whereas the other polymorph ($\gamma$ phase) is photostable. There are well-established correlations[139–141] between the structural properties and photoreactivities of a wide range of derivatives of *trans*-cinnamic acid in the solid state. It was therefore of much interest when the structure (from single-crystal X-ray diffraction) of the photoreactive $\beta$ phase of *p*-FCA was reported[149] to represent an exception to these well-established correlations. However, it was shown subsequently[148]

(Figure 19) that the powder X-ray diffraction pattern calculated using this reported structure is actually in agreement with the experimental powder X-ray diffraction pattern of the photostable $\gamma$ phase of *p*-FCA. Therefore, the crystal structure reported from single-crystal X-ray diffraction to be the

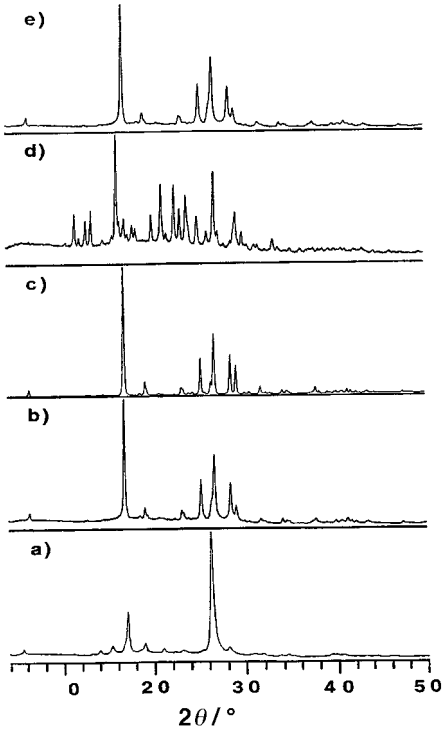


Figure 19. Powder X-ray diffraction patterns:[148] a) recorded for a sample of *p*-FCA crystallized from ethanol ($\beta$ phase); b) recorded for a sample of *p*-FCA crystallized from acetone ($\gamma$ phase); c) simulated on the basis of the crystal structure reported in ref [149]; d) recorded for the sample of *p*-FCA crystallized from ethanol ($\beta$ phase) following UV irradiation; e) recorded for the sample of *p*-FCA crystallized from acetone ($\gamma$ phase) following UV irradiation.

$\beta$ phase of *p*-FCA was actually the structure of the $\gamma$ phase (and therefore did not represent a structurally anomalous photoreactive *trans*-cinnamic acid derivative). Thus, the actual single crystal ($\gamma$ phase) selected for the single-crystal diffraction study in the original work[149] was not representative of the bulk material ($\beta$ phase). This example demonstrates clearly the importance of using powder diffraction data to confirm that a structure determined from single-crystal data is actually representative of the bulk polycrystalline sample. Other examples of the importance of adopting this strategy have been noted.[150–152]

In summary, while new and improved radiation sources (both laboratory-based X-ray sources and new generations of synchrotron sources) may be expected to continue to allow single crystals of smaller and smaller size to be investigated by single-crystal diffraction methods in the future, there are clear areas of application in which powder diffraction techniques are essential. Furthermore, in spite of the advances that have allowed single-crystal diffraction experiments to be carried out on micro-crystals, there remains a significant range of materials for which the crystallite sizes are too small to be physically handled as single crystals (e.g. in single-crystal diffraction experiments), but sufficiently large to give powder diffraction patterns of good quality.

## 5. Overview of Techniques Used in Structure Determination from Powder Diffraction Data

### 5.1. Indexing

As discussed in Section 2.1, the first stage of crystal-structure determination from powder diffraction data involves determination of the unit cell dimensions ($a$, $b$, $c$, $\alpha$, $\beta$, $\gamma$) by "indexing" the powder diffraction pattern (although the unit-cell dimensions may sometimes be known independently—for example, from electron diffraction data). Clearly it is possible to proceed with structure solution and refinement only if the correct unit cell is found at this stage. Unfortunately, difficulties encountered in the reliable indexing of powder diffraction patterns using existing techniques is often found to be the limiting step in the structure determination process.

The most widely used programs for indexing powder diffraction data (ITO,[153] TREOR,[154] DICVOL,[155] and CRYSFIRE[156]) all consider the measured positions of peak maxima for a number (usually about 20) of selected peaks. General reviews are given in refs. [157–159]. In contrast to recent advances in techniques for structure solution, there has been relatively little fundamental development of indexing methods since the pioneering work several years ago.

As already mentioned, experimental powder diffraction patterns typically have considerable peak overlap and sometimes peak displacements, which can lead to problems in indexing using the methods described above. For example, certain peaks which may be crucial for correct indexing may be obscured or completely unresolved because of peak overlap. Another problem arises when an impurity phase (or a second polymorph of the material of interest) is present within the powder sample, and often constitutes an intractable problem for indexing by existing methods (unless the presence of the impurity phase(s) is known in advance). Indexing can also fail if there is significant zero-point error in the detector or poor definition of peak positions because of poor sample crystallinity or poor instrumental resolution.

Given the clear requirement for new indexing strategies, methods that use all regions of the powder diffraction pattern (including the overlapped peaks) are particularly appealing. On this basis, a new indexing strategy based on whole-profile fitting and global optimization using a genetic algorithm has been developed recently.[160] In this method, trial unit cells ($a$, $b$, $c$, $\alpha$, $\beta$, $\gamma$) are generated using a genetic-algorithm strategy, and the quality of each trial unit cell is assessed using a whole-profile fitting procedure. A method for indexing powder diffraction data using a genetic algorithm within the conventional indexing strategy (i.e. requiring a set of extracted peak positions) has also been proposed.[161]

After the powder diffraction pattern has been indexed successfully, the space group may be assigned by identifying the conditions for systematic absences. If the space group

cannot be assigned uniquely, structure-solution calculations should be carried out separately for each of the plausible space groups. Knowledge of the unit-cell volume and space group, together with density considerations, should allow the contents of the asymmetric unit to be established. Information obtained from other experimental techniques (for example, high-resolution solid-state NMR spectroscopy) may be particularly helpful in confirming the number of molecules and/or structural units in the asymmetric unit.

## 5.2. Powder Diffraction Profiles

### *5.2.1. Definition of a Powder Diffraction Profile*

The complete powder diffraction profile (either for an experimental or calculated powder diffraction pattern) may be described in terms of the following components: 1) the peak positions (which depend on the unit-cell dimensions), 2) the peak intensities (which depend on the positions of atoms in the unit cell, and atomic-displacement parameters), 3) the peak shapes and peak widths (which may be described using $2\theta$-dependent analytical functions), and 4) the background intensity distribution. The peak shape depends on characteristic properties of both the instrument and the sample, and different peak-shape functions are appropriate under different circumstances. The most common peak shape for powder X-ray diffraction is the pseudo-Voigt function,[162] which represents a hybrid of Gaussian and Lorentzian character, although several other types of peak-shape function may be applicable under different circumstances. These peak shapes and the types of analytical functions that are commonly used to describe the $2\theta$ dependence of the peak width are described in detail elsewhere.[4]

### *5.2.2. Analysis of Powder Diffraction Profiles Prior to Structure Solution*

As discussed in Section 2.2, traditional techniques (as well as some implementations of direct-space techniques, as discussed in Section 2.3) for structure solution from powder diffraction data require a set of accurate intensities of individual reflections extracted directly from the experimental powder diffraction pattern (through so-called "pattern decomposition" methods, such as the techniques of Pawley and Le Bail (reviewed in ref. [1]), which involve fitting the complete powder diffraction profile to establish the intensities of each of the underlying diffraction maxima). Advances in the techniques for peak extraction in this regard have been referenced in Section 2.2.

As discussed in Section 2.3, most implementations of direct-space structure-solution methods have used a profile-based figure-of-merit (such as $R_{wp}$), and therefore do not use the intensities of individual reflections extracted from the powder diffraction pattern. However, for such direct-space techniques, analysis of the powder diffraction pattern prior to structure solution is also very important. With such figures-of-merit, a reliable comparison between calculated and experimental powder diffraction patterns requires that the parameters defining the peak positions (unit-cell parameters and zero-point offset), the peak shape (peak width, peak-shape function and peak-mixing parameters) and the background intensity distribution used in calculating the powder diffraction pattern for each trial structure accurately reflect those in the experimental powder diffraction pattern. It is clearly of paramount importance that reliable values of these parameters are established *prior to* the structure-solution calculation, requiring detailed analysis of the powder diffraction profiles in the experimental powder diffraction pattern. In general, this step is carried out either by peak-shape fitting of a few selected peaks, or by procedures for fitting the whole powder diffraction pattern by refinement of the parameters (see Section 5.2.1) that define the profile. Such fitting of the complete experimental powder diffraction profile should involve refinement of the unit-cell parameters, the background intensity distribution, zero-point shift parameters, peak-width parameters, and peak-shape parameters, *with the use of arbitrary peak intensities* (i.e. without using any structural model to determine the peak intensities). Careful prior analysis of the experimental data in this way ensures that the profile parameters used subsequently in structure-solution calculations provide a reliable description of the experimental powder diffraction pattern.

## 5.3. New Strategies for Structure Solution

Over recent years, there has been substantially increasing interest in the opportunities to determine crystal structures directly from powder diffraction data, and an ever increasing number of different types of materials have been studied (as discussed in Section 3). In terms of structure determination of molecular solids from powder diffraction data, for example, the recent advances have resulted largely from the development of direct-space techniques for structure solution. Although the application of these methods is not confined to molecular solids, these techniques have already made great impact in the study of organic molecular materials for which traditional approaches for powder structure solution have generally had limited success. Here we provide more details of the methodology underlying direct-space techniques for structure solution, recognizing that the methodology underlying traditional techniques has been reviewed extensively elsewhere.[1, 6–13]

### *5.3.1. The Structural Fragment*

In the direct-space approach, each trial crystal structure is defined by a set of variables $\Gamma$, representing the position, orientation, and intramolecular geometry of the structural fragment. The choice of structural fragment for any particular problem is not necessarily unique. For the general case of a rigid molecule, six variables are required: $\Gamma = \{x, y, z, \theta, \phi, \psi\}$. For the general case of a molecule with a number ($n$) of unknown torsion angles $\tau_i$, the structural fragment is defined by ($6+n$) variables: $\Gamma = \{x, y, z, \theta, \phi, \psi, \tau_1, \tau_2, \ldots \tau_n\}$. When the molecules occupy special positions in the crystal structure, the number of variable degrees of freedom is reduced. For example, when a molecular inversion center resides on a crystallographic inversion center, the molecule has no trans-

lational degrees of freedom, and there are $(3+m)$ variables: $\Gamma=\{\theta, \phi, \psi, \tau_1, \tau_2,\ldots\tau_m\}$ (where $m$ is the number of variable torsion angles in half the molecule)—see the example discussed in Section 3.7. For the case of two or more molecules in the asymmetric unit (for example, cocrystals), the structural fragment comprises a separate set of variables $\Gamma$ for each molecule—see the example discussed in Section 3.1.

As discussed in Sections 2.4 and 3, other structural information or knowledge can be used in conjunction with direct-space approaches to reduce the extent of parameter space that needs to be searched in the structure-solution calculation. For example, regions of parameter space that correspond to unreasonably short contacts between nonbonded atoms or between independent molecules in the unit cell may be excluded from the direct-space search procedure (although, in the case of Monte Carlo and simulated annealing methods, care must be taken to ensure that the excluded regions of parameter space do not restrict plausible pathways leading towards the correct structure).

In general, the complexity of direct-space structure-solution calculations increases as the number of variables required to define the structural fragment increases (i.e. as the number of degrees of freedom in the global-optimization calculation increases). While the majority of applications of direct-space structure solution have included the complete asymmetric unit (with hydrogen atoms usually omitted) in the structural fragment, some applications have sought rational approaches for reducing the number of degrees of freedom. For example, in the structure solution of $p$-$BrC_6H_4CH_2CO_2H$ using the Monte Carlo method,[33] two separate calculations were carried out: in the first calculation, translation of the dominant scatterer (Br atom) within the unit cell was determined, and then after establishing the correct position of the Br atom, reorientation of the -$C_6H_4CH_2$ part of the molecule around the fixed position of the Br atom found in the first calculation.

Another approach that has been used to simplify the structural fragment within the context of direct-space structure solution is the so-called "pseudo-atom" method. This strategy has been applied in a number of cases for structure solution of coordination compounds.[163, 164] In the first stages of structure solution, cyclic fragments in these structures were each represented by a single pseudo-atom (with similar total scattering power), allowing the center-of-gravity of each of the cyclic fragments to be approximately located. Subsequently, the complete cyclic fragments were introduced in the calculation at the positions located by the pseudo-atoms, to determine their orientations, with only limited translation of the fragments allowed.

### 5.3.2. Grid Search Methods

The most straightforward (but least efficient) direct-space approach for structure solution is based on a grid search procedure, in which the molecule is moved systematically throughout the unit cell. Thus, by changing the values of the variables in the set $\Gamma$ using predefined grid increments in each variable, all possible packing arrangements for the system of interest are assessed systematically. This exhaustive search procedure can be very demanding computationally, even when the number of variables is relatively modest, and consequently the study of conformationally flexible molecules may be prohibitively time consuming by this approach. For this reason, most structure-solution problems tackled using grid search procedures have been cases in which the structural fragment has comprised a dominant scatterer or a rigid molecule[42, 44, 45, 123, 134] although the study of a system with some conformational flexibility has been reported.[43]

### 5.3.3. Monte Carlo and Simulated Annealing Techniques

The foundations of the Monte Carlo and simulated-annealing techniques[165–167] are very closely related, and both involve the generation of a sequence of structures (each denoted $\Gamma_i$ for $i=1, 2,\ldots j, j+1,\ldots N$) for consideration as potential structure solutions. We begin by focusing on the Monte Carlo method, as implemented first in ref. [33] and applied subsequently to a wide variety of problems[39, 54, 60, 75, 76, 91, 138, 144]. Each structure generated during the Monte Carlo calculation is derived from the previous structure by a random displacement of the structural fragment within the unit cell. The procedure for each Monte Carlo move (described here for the general case in which structure $\Gamma_{j+1}$ is generated from structure $\Gamma_j$) comprises the following steps (see Figure 20).

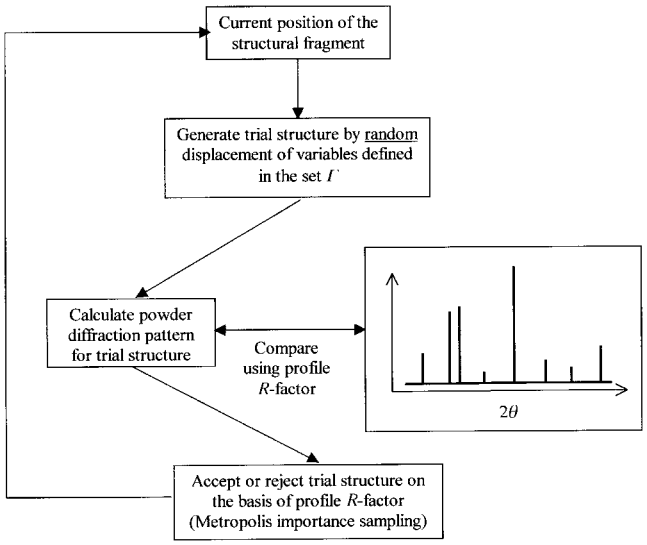


Figure 20. Summary of the steps involved in carrying out an individual Monte Carlo "move".

1) Starting from structure $\Gamma_j$, a trial structure $\Gamma_{j,T}$ is generated by making small random displacements to each of the variables in the set $\{x, y, z, \theta, \phi, \psi, \tau_1, \tau_2,\ldots\tau_n\}$ (or in some cases a subset of these variables). The agreement between the powder diffraction pattern calculated for the trial structure and the experimental powder diffraction pattern is then assessed, for example using $R_{wp}$.

2) The trial structure is then accepted or rejected by considering the difference $Z=R_{wp}(\Gamma_{j,T})-R_{wp}(\Gamma_j)$ between the values of $R_{wp}$ for structures $\Gamma_{j,T}$ and $\Gamma_j$ and invoking the importance sampling algorithm developed by Metropolis et al.[165] If $Z\leq 0$, the trial structure is automatically accepted,

whereas if $Z > 0$, the trial structure is accepted with probability $\exp(-Z/S)$ and rejected with probability, $[1 - \exp(-Z/S)]$, where $S$ is an appropriate scaling factor. If the trial structure is accepted, structure $\Gamma_{j+1}$ is taken to be the same as $\Gamma_{j,T}$. If the trial structure is rejected, structure $\Gamma_{j+1}$ is taken to be the same as $\Gamma_j$. The parameter $S$ may be fixed or may be varied in a controlled manner during the calculation. Clearly the higher the value of $S$, the greater the probability that trial structures with $Z > 0$ will be accepted (note that $S$ operates in a manner analogous to temperature in applications of Monte Carlo techniques in energy simulations).

The above procedure is repeated to generate a large number of structures, with each structure derived from the previous one through small random displacements in the values of the structural variables in the set $\Gamma$. Figure 21 shows

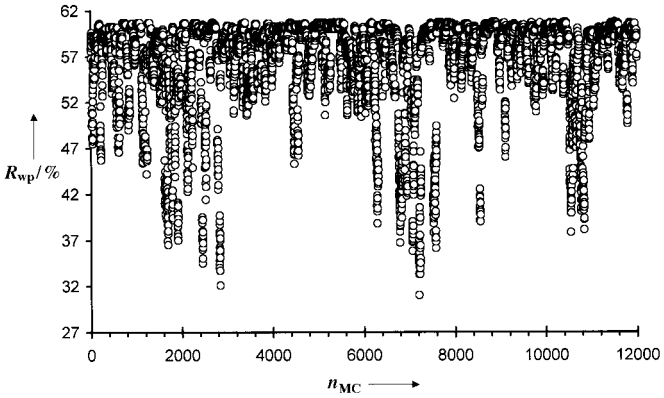


Figure 21. A typical plot of $R_{wp}$ for trial structures generated in a Monte Carlo structure solution calculation versus the corresponding Monte Carlo move number $n_{MC}$.

a typical plot of $R_{wp}$ for trial structures generated in a Monte Carlo structure-solution calculation as a function of Monte Carlo move number. After a sufficiently wide-range of parameter space has been explored, the best structure solution (corresponding to lowest $R_{wp}$) is used as the starting model for structure refinement. It is important to emphasize that the Monte Carlo method does not represent minimization of $R_{wp}$ (except if $S = 0$), but explores parameter space in a manner that gives emphasis to regions with ow $R_{wp}$, but with the ability to escape from local minima in $R_{wp}$.

The fundamental difference between Monte Carlo and simulated-annealing techniques concerns the way in which the parameter $S$ is used to control the sampling algorithm. In the Monte Carlo method, $S$ may be fixed or varied manually, whereas in simulated annealing, $S$ is decreased systematically according to an annealing schedule or temperature-reduction procedure.[167] A detailed description of the methodology underlying some simulated-annealing methods is given in refs. [32, 36]. The simulated-annealing method was first used in structure determination from powder diffraction data to solve the previously known crystal structure of benzene from simulated powder diffraction data.[34] Although this example concerned a rigid molecule of high symmetry, the problem was complicated by the assumption of space group $P1$, which requires the positions and orientations of all four molecules in the unit cell to be found independently. The simulated-annealing technique has since been applied to real experimental powder diffraction data in cases of rigid[35] and flexible[36–38, 41, 91] molecules. Details of the simulated-annealing methods adopted differ in several respects, including details of the temperature-reduction procedure and definition of the figure-of-merit.

### 5.3.4. Genetic-Algorithm Technique

Genetic Algorithms[168–170] are optimization techniques based on the principles of natural evolution, and involve the familiar evolutionary operations of mating, mutation, and natural selection. By natural selection, the fittest members of a population survive and procreate, leading to improved individuals in subsequent generations, and leading ultimately to the optimal individual.

The possibility of using genetic-algorithm techniques in structure solution from powder diffraction data was realized independently by two research groups. Our approach[46, 48, 49, 53, 57, 72, 84, 85, 171, 172] and the approach of Shankland, David and coworkers[47, 71, 173] differ in the definition and handling of the fitness function, as well as other aspects of the way in which the genetic algorithm is implemented. Details can be found in the papers cited. A schematic flow-chart of our implementation of the genetic algorithm[49] is shown in Figure 22.

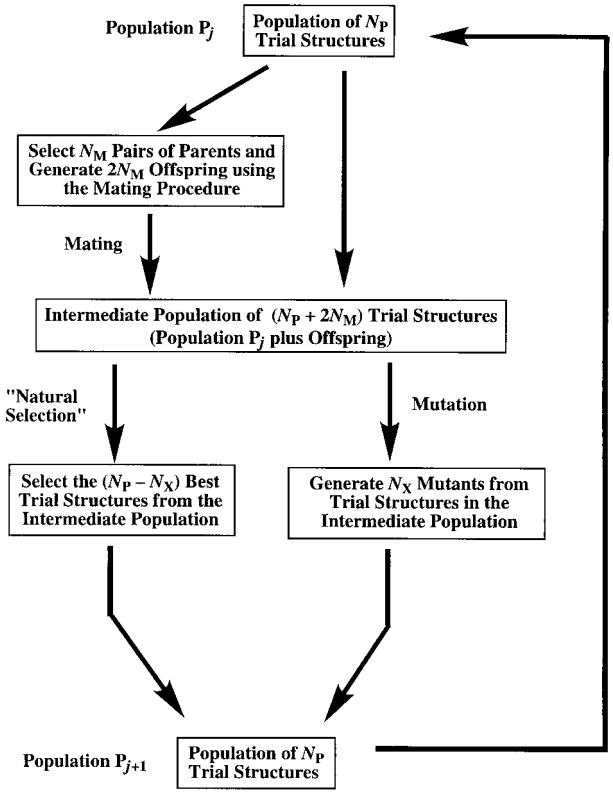


Figure 22. Flow chart representing the evolution of the population from one generation (population $P_j$) to the next generation (population $P_{j+1}$) in the genetic algorithm for powder structure solution.[49]

In the genetic-algorithm approach for structure solution, the evolution of a population of trial crystal structures is investigated. Each member of the population is uniquely characterized by the set of variables $\Gamma$ (see Section 5.3.1), and the set $\Gamma$ can be regarded to define its "genetic code". The initial population $P_o$ contains $N_p$ randomly generated structures, and the population then evolves through subsequent generations by applying the evolutionary operations of mating, mutation, and natural selection. The number $N_p$ of structures in the population is constant for all generations, and $N_M$ mating operations and $N_X$ mutation operations are performed in the evolution of the population from one generation to the next.

The probability that a given structure survives into subsequent generations, and the probability that it takes part in mating, depend on its fitness. In our implementation of the genetic algorithm,[49] the fitness of a structure is defined as a function of its weighted profile $R$ factor $R_{wp}$, and fitness therefore measures how well the structure agrees with the experimental powder diffraction data. A number of fitness functions $F(\rho)$ have been used, where it is convenient to use the scaled $R$ factor $\rho = [R_{wp} - R_{min}]/[R_{max} - R_{min}]$, with $R_{min}$ and $R_{max}$ representing the lowest and highest values of $R_{wp}$ in the current population, respectively. The values of $R_{min}$ and $R_{max}$ are continually updated as the population evolves during the genetic-algorithm calculation, representing "dynamic scaling" of the fitness function.

Before each mating operation, a structure (with fitness $F$) is chosen from the population at random and is allowed to participate in mating if $F > \Re$, where $\Re$ is a random number generated between 0 and 1. A second structure is then found using the same selection procedure, and the two structures are allowed to mate with each other. This procedure is repeated until $N_M$ pairs of parents have been selected. Mating (crossover) between two selected parents is carried out by combining the genetic codes of the two parents, although the actual strategy used depends on the complexity of the structural fragment. As an example, for a structural fragment with two torsional degrees of freedom, one method for mating involves partitioning the eight variables that define each structure into four groups $\{x,y,z \mid \theta,\phi,\psi \mid \tau_1 \mid \tau_2\}$. Two offspring are then generated, with each offspring taking two complementary groups from each parent. This operation may be carried out in three different (but equiprobable) ways from a given pair of parents, and thus mating the parents $\{x_a,y_a,z_a \mid \theta_a,\phi_a,\psi_a \mid \tau_{1a} \mid \tau_{2a}\}$ and $\{x_b,y_b,z_b \mid \theta_b,\phi_b,\psi_b \mid \tau_{1b} \mid \tau_{2b}\}$ leads with equal probability to one of the following pairs of offspring:

- $\{x_a,y_a,z_a \mid \theta_a,\phi_a,\psi_a \mid \tau_{1b} \mid \tau_{2b}\}$ and $\{x_b,y_b,z_b \mid \theta_b,\phi_b,\psi_b \mid \tau_{1a} \mid \tau_{2a}\}$
- $\{x_a,y_a,z_a \mid \theta_b,\phi_b,\psi_b \mid \tau_{1a} \mid \tau_{2b}\}$ and $\{x_b,y_b,z_b \mid \theta_a,\phi_a,\psi_a \mid \tau_{1b} \mid \tau_{2a}\}$
- $\{x_a,y_a,z_a \mid \theta_b,\phi_b,\psi_b \mid \tau_{1b} \mid \tau_{2a}\}$ and $\{x_b,y_b,z_b \mid \theta_a,\phi_a,\psi_a \mid \tau_{1a} \mid \tau_{2b}\}$

Many other methods for mating the two parents may be implemented, each with specific advantages under particular circumstances.

Each mating operation leads to two offspring, giving a total of $2N_M$ offspring in each generation. These offspring together with all $N_p$ structures from the previous generation give rise to an intermediate population of $(N_p+2N_M)$ structures. These structures are then ranked according to fitness in preparation for the natural-selection process (see below). If two or more structures are identical within predefined tolerance limits, all but one of these structures is eliminated from the intermediate population.

In each generation, some mutant structures are also generated to maintain diversity within the population (note that mutations create new genetic material within the population, whereas mating redistributes the existing genetic material). For mutation, $N_X$ structures are selected at random from the intermediate population, and mutants are generated from these structures by making random changes to one or more variables in the set $\Gamma$. These changes may be new random values (static mutation) or small random displacements from the existing value (dynamic mutation). It is important to note that the "parent" structures used to create the mutants are not replaced by the mutants, but remain within the intermediate population.

As shown in Figure 22, the next generation is constructed by taking the $(N_p - N_X)$ members of highest fitness from the intermediate population (analogous to "natural selection" in biological evolution) together with the $N_X$ mutant structures generated from the intermediate population. On passing from one generation to the next, the best structure in the population (corresponding to $R_{min}$) must either improve or remain the same, and the overall quality of the population (assessed from the average value of $R_{wp}$) usually improves. Figure 11 shows a typical plot of the evolution of $R_{wp}$ for the best structure in the population and the average value of $R_{wp}$ for the structures in the population as a function of generation number in a genetic-algorithm structure-solution calculation.

The evolutionary cycle shown in Figure 22 is repeated for a specified number of generations or until convergence is reached. Typically, our genetic-algorithm structure-solution calculations have involved a population size ($N_P$) of a hundred (or fewer) structures, and typically 50 to 100 mating operations ($N_M$) and 10 to 20 mutation operations ($N_X$) are carried out in each generation. In general, a few hundred generations are usually sufficient to obtain the correct structure solution.

In our most recent implementation of the genetic-algorithm method,[85] each new structure generated during the calculation is subjected to local minimization of $R_{wp}$ with respect to the structural variables in the set $\Gamma$, and only these minimized structures are used subsequently in the evolution of the population. Introduction of local minimization in this way improves the efficiency of the calculation in terms of a significant reduction in the number of generations required to find the correct structure solution. Furthermore, the reliability and reproducibility in terms of finding the correct structure solution (for example, in repeated runs from different random initial populations) are also substantially improved. These advantages of introducing local minimization of $R_{wp}$ may be attributed to a favorable combination of stochastic (i.e. the genetic algorithm) and deterministic (i.e. the minimization) components within the global-optimization strategy. As the genetic characteristics of each structure sampled on the $R_{wp}$ hypersurface become modified in the minimization step depending on the nature of its local environment, the genetic algorithm incorporating local minimization represents Lamarckian (rather than Darwinian) evolution.

In comparison with other approaches for global optimization, we note that genetic-algorithm methods simultaneously investigate different regions of parameter space. Furthermore, information from different regions of parameter space is passed actively between different members of the population by the mating operation. In implementing genetic-algorithm techniques, there is considerable scope for diversity in the methods and rules for carrying out the different evolutionary operations and in the definition of the fitness function. Furthermore, details of the flow-chart shown in Figure 22 may differ from one implementation to another. To fully understand how to optimize the genetic-algorithm approach for particular types of structural problem or particular sets of diffraction data, it is necessary to consider and assess a wide-range of strategies for carrying out the different evolutionary operations.[49, 174]

#### 5.3.5. Combinations of Techniques

Direct-space approaches have also been used in combination with other techniques to facilitate structure solution. An example concerns the use of structure envelopes to reduce considerably the region to be explored by direct-space techniques and hence the computer time required to solve the structure. One such approach is based on a combination of the maximum entropy and likelihood method[175] and the Monte Carlo method, and has been used to study organic materials.[69] The maximum entropy and likelihood method is used to generate an electron-density map which establishes the regions of the asymmetric unit in which the molecule is most likely to be located. At lower than atomic resolution, this map is then investigated visually and a molecular model is fitted to the electron-density map. The structural model generated in this way is then modified within the structure envelope by means of a Monte Carlo calculation.

In a related approach, the structure envelope is defined by a periodic nodal surface generated from a few strong low-index reflections extracted from the powder diffraction pattern followed by exploration of this region of parameter space by using a grid search procedure.[106] The success of this procedure has been demonstrated for organic and ionic materials as well as zeolite structures. In some cases, the initial fit of the model to the structure envelope is sufficiently good to allow Rietveld refinement to proceed directly, without the need for subsequent improvement using a direct-space structure solution calculation.

### 5.4. Rietveld Refinement

In Rietveld refinement of a crystal structure from powder diffraction data,[3, 4] every point in the digitized powder diffraction profile is considered as an individual intensity measurement. In Rietveld refinement, the calculated powder diffraction pattern is compared, point by point, with the experimental powder diffraction pattern, and selected parameters defining the structural model and/or the profile are adjusted by least-squares methods to obtain an optimal fit between the experimental and calculated powder diffraction patterns. Several criteria can be used[4, 162] to assess the agreement between the experimental and calculated powder diffraction patterns, and the most common figure-of-merit is the weighted profile $R$ factor $R_{wp}$. Some commonly used programs for Rietveld refinement are GSAS,[176] FULLPROF,[177] PROFIL,[178] DBW,[179] and RIETAN.[180]

For successful Rietveld refinement, the initial structural model (from the structure solution) must be a sufficiently good representation of the correct structure. As Rietveld refinement can often suffer from problems of instability, it is generally necessary to use geometric restraints (soft constraints) based on standard molecular geometries to bias the refinement towards structurally reasonable results and to prevent excessive shifts in the atomic positions. In general, the introduction of restraints allows more parameters to be refined than would be possible in unrestrained refinement from the same experimental data, and indeed refinement is often successful only if appropriate restraints are imposed.

### 5.5. Other Considerations

General experimental factors relating to the measurement of powder diffraction data have been reviewed elsewhere,[11] and here we highlight only certain selected aspects.

First, we consider the relative merits of using synchrotron X-ray powder diffraction data versus conventional laboratory powder X-ray diffraction data (see also Section 2.4), recognizing that the good vertical collimation and high brightness of synchrotron radiation lead to powder diffraction data of higher resolution and often of improved signal/noise ratio. With high resolution, problems arising from peak overlap can be alleviated to some extent, allowing less ambiguity in the intensities of individual reflections extracted from the powder diffraction pattern. In this regard, synchrotron radiation is generally advantageous when traditional techniques (or a direct-space technique using a figure-of-merit based on extracted intensities) are to be used for structure solution. The higher resolution of synchrotron data may also be particularly advantageous at the stage of indexing the powder diffraction pattern. As discussed in Section 3, however, much successful structure determination has been achieved using conventional laboratory powder X-ray diffraction data, and in general, the use of synchrotron data is essential only in certain specific cases.

Second, structure solution from powder diffraction data has a good chance of success only if the experimental powder diffraction pattern contains reliable information on the intrinsic relative intensities of the diffraction maxima, which requires that there is no substantial "preferred orientation" in the powder sample. Preferred orientation arises when the crystallites in the powder are oriented preferentially in certain directions, and can be particularly severe when the crystal morphology is strongly anisotropic (e.g. long needles or flat plates). When there is a nonrandom distribution of crystallite orientations in the sample, the measured relative peak intensities differ from the intrinsic relative diffraction intensities, limiting the prospects for determining reliable structural information from the powder diffraction pattern. The existence of preferred orientation can be detected by meas-

uring powder diffraction data for the same sample in different sample holders (e.g. capillary versus flat sample) or for different measurement geometries (e.g. reflection versus transmission). Experimental approaches for reducing the extent of preferred orientation include the use of a capillary or end-loading sample holder, mixing the sample with an amorphous material, spray-drying, or appropriate grinding to induce a crystal morphology that is as isotropic as possible. For experimental data affected by preferred orientation, corrections can be made during structure refinement[181] once a sufficiently good structural model is known. Methods have also been reported[182, 183] for the early detection of preferred orientation (by mathematical means) and the application of corrections based on statistical analysis of extracted intensities.

In general, direct-space structure solution techniques are probably more robust than traditional techniques when the experimental data are affected by preferred orientation, presumably because a substantial amount of structural knowledge is already input into the calculation through the use of a structural fragment. Thus, the Monte Carlo method has led to the successful structure determination of benzoic acid,[184] 5-bromonicotinic acid,[185] and the 1:1 cocrystal formed between 1,2,3-trihydroxybenzene and hexamethylenetetramine[60] from experimental powder diffraction data known to be significantly affected by preferred orientation. In these cases the structure solution process was carried out in the normal manner and corrections for preferred orientation were only introduced at the refinement stage.

## 6. Concluding Remarks

The techniques and methods presented here for structure determination from powder diffraction data represent powerful additions to the range of experimental techniques that may be used for structure determination of solids. In recent years, significant advances in the opportunities for structure determination from powder diffraction have arisen mainly from advances in techniques for overcoming the intrinsic problems encountered in the structure-solution stage of the structure-determination process. The examples highlighted in this article represent a contemporary snapshot of the current status of this field, and there is every reason to be confident that the progress made in recent years (illustrated in Figure 3) will continue long into the future. Thus, the future application of the techniques that are now available promises to reveal new and important insights in several areas for which structural characterization by single-crystal diffraction techniques has hitherto proven intractable.

Looking towards the future, continued advances in the capabilities and efficiencies of the techniques used at each stage of the structure-determination process, coupled with continual improvements in the instrumentation for data collection and in the speed of computers for data analysis, will allow existing problems to be tackled more routinely and will extend the boundaries of the methodology towards larger and more challenging problems. Undoubtedly the ultimate aim is to extend the application of powder diffraction techniques into the biological arena, and the recent demonstration[186] of the successful refinement of a *known* protein structure (the 1261-atom protein metmyoglobin) from synchrotron X-ray powder diffraction data provides a glimpse of future possibilities for the complete structure determination of new protein structures from powder diffraction data. While substantial further development and optimization of techniques for structure solution are required before this dream may become a reality, it is nevertheless relevant to note that, in the field of molecular crystallography, the current scope of powder diffraction techniques for complete structure determination is somewhat comparable to the state-of-the-art in single-crystal diffraction around the 1950s.[187] We may forecast with optimism that the future evolution in the capabilities of powder diffraction techniques for structure determination will mirror the developments that have taken place in the capabilities of single-crystal diffraction techniques in the last 50 years.

*We are indebted to several colleagues and collaborators, particularly Dr. Roy Johnston and others mentioned in the references, for discussions and collaboration in the areas of research described in this paper. We are grateful to the following organizations for providing financial support for our research in this field: EPSRC, the University of Birmingham, Ciba Specialty Chemicals, the Nuffield Foundation, Molecular Simulations (MSI), Daresbury Laboratory, GlaxoSmithKline plc and Wyeth Ayerst Ltd. M.T. is grateful to the Royal Society for the award of a University Research Fellowship.*

Received: February 8, 2000 [A 393]

[1] K. D. M. Harris, M. Tremayne, *Chem. Mater.* **1996**, *8*, 2554.
[2] A. K. Cheetham in *Solid State Chemistry Techniques* (Eds.: A. K. Cheetham, P. Day), Oxford University Press, Oxford, pp. 39–83, **1987**.
[3] H. M. Rietveld, *J. Appl. Crystallogr.* **1969**, *2*, 65.
[4] *The Rietveld Method* (Ed.: R. A. Young), International Union of Crystallography and Oxford University Press, Oxford, **1993**.
[5] There are two types of overlap of peaks in a powder diffraction pattern: 1) "accidental" overlap of nonequivalent reflections for which the peak positions (i.e. $2\theta$ values or $d$-spacings) happen to be close to each other; this type of overlap is particularly prevalent at high diffraction angles, and can be particularly severe for low-symmetry structures; and 2) systematic overlap of well-defined groups of nonequivalent reflections, for which the peak positions are identical because of symmetry, but with no symmetry-imposed relationship between the intensities of these reflections (this situation occurs only for certain high-symmetry structures; e.g. for reflections $\{hkl\}$ and $\{khl\}$ in a tetragonal system with Laue group $4/m$, $d(hkl) = d(khl)$ but $I(hkl) \neq I(khl)$).
[6] A. N. Christensen, M. S. Lehmann, M. Nielsen, *Aust. J. Phys.* **1985**, *38*, 497.
[7] A. K. Cheetham, A. P. Wilkinson, *J. Phys. Chem. Solids* **1991**, *52*, 1199.
[8] L. B. McCusker, *Acta Crystallogr. Sect. A* **1991**, *47*, 297.
[9] A. K. Cheetham, A. P. Wilkinson, *Angew. Chem.* **1992**, *104*, 1594; *Angew. Chem. Int. Ed. Engl.* **1992**, *31*, 1557.
[10] P. R. Rudolf, *Mater. Chem. Phys.* **1993**, *35*, 267.
[11] J. I. Langford, D. Louër, *Rep. Progr. Phys.* **1996**, *59*, 131.
[12] D. M. Poojary, A. Clearfield, *Acc. Chem. Res.* **1997**, *30*, 414.
[13] A. Meden, *Croat. Chem. Acta* **1998**, *71*, 615.
[14] J. D. Dunitz, *X-ray Analysis and the Structures of Organic Molecules*, VHCA, Basel, **1995**.

[15] J. P. Glusker, K. N. Trueblood, *Crystal Structure Analysis—A Primer*, Oxford University Press, Oxford, **1985**.
[16] W. I. F. David, *J. Appl. Crystallogr.* **1987**, *20*, 316.
[17] W. I. F. David, *Nature* **1990**, *346*, 731.
[18] J. Jansen, R. Peschar, H. Schenk, *J. Appl. Crystallogr.* **1992**, *25*, 237.
[19] M. A. Estermann, L. B. McCusker, C. Baerlocher, *J. Appl. Crystallogr.* **1992**, *25*, 539.
[20] R. W. Cheary, A. A. Coelho, *J. Appl. Crystallogr.* **1992**, *25*, 109.
[21] M. A. Estermann, V. Gramlich, *J. Appl. Crystallogr.* **1993**, *26*, 396.
[22] C. J. Gilmore, K. Shankland, G. Bricogne, *Proc. R. Soc. London A* **1993**, *442*, 97.
[23] D. S. Sivia, W. I. F. David, *Acta Crystallogr. Sect. A* **1994**, *50*, 703.
[24] C. J. Gilmore, *Acta Crystallogr. Sect. A* **1996**, *52*, 561.
[25] W. I. F. David, *J. Appl. Crystallogr.* **1999**, *32*, 654.
[26] A. Altomare, M. C. Burla, M. Camalli, B. Carrozzini, G. L. Cascarano, C. Giacovazzo, A. Guagliardi, A. G. G. Moliterni, G. Polidori, R. Rizzi, *J. Appl. Crystallogr.* **1999**, *32*, 339.
[27] J. Jansen, R. Peschar, H. Schenk, *Z. Kristallogr.* **1993**, *206*, 33.
[28] J. Rius, *Powder Diffr.* **1999**, *14*, 267.
[29] J. Rius, C. Miravitlles, *J. Appl. Crystallogr.* **1988**, *21*, 224.
[30] J. Sane, J. Rius, T. Calvet, M. A. Cuevas-Diarte, *Acta Crystallogr. Sect. B* **1997**, *53*, 702.
[31] K. D. M. Harris, *J. Chin. Chem. Soc.* **1999**, *46*, 23.
[32] C. M. Freeman, A. M. Gorman, J. M. Newsam in *Computer Modelling in Inorganic Crystallography* (Ed.: C. R. A. Catlow), Academic Press, San Diego, **1997**.
[33] K. D. M. Harris, M. Tremayne, P. Lightfoot, P. G. Bruce, *J. Am. Chem. Soc.* **1994**, *116*, 3543.
[34] "Accuracy in Powder Diffraction II": J. M. Newsam, M. W. Deem, C. M. Freeman, *NIST Spec. Publ.* **1992**, *846*, 80–91.
[35] D. Ramprasad, G. B. Pez, B. H. Toby, T. J. Markley, R. M. Pearlstein, *J. Am. Chem. Soc.* **1995**, *117*, 10694.
[36] G. E. Engel, S. Wilke, O. König, K. D. M. Harris, F. J. J. Leusen, *J. Appl. Crystallogr.* **1999**, *32*, 1169.
[37] Y. G. Andreev, P. Lightfoot, P. G. Bruce, *J. Appl. Crystallogr.* **1997**, *30*, 294.
[38] W. I. F. David, K. Shankland, N. Shankland, *Chem. Commun.* **1998**, 931.
[39] M. Tremayne, B. M. Kariuki, K. D. M. Harris, *Angew. Chem.* **1997**, *109*, 788; *Angew. Chem. Int. Ed. Engl.* **1997**, *36*, 770.
[40] K. D. M. Harris, B. M. Kariuki, M. Tremayne, *Mater. Sci. Forum* **1998**, *278–291*, 32.
[41] Y. G. Andreev, P. Lightfoot, P. G. Bruce, *Chem. Commun.* **1996**, 2169.
[42] G. Reck, R.-G. Kretschmer, L. Kutschabsky, W. Pritzkow, *Acta Crystallogr. Sect. A* **1988**, *44*, 417.
[43] R. B. Hammond, K. J. Roberts, R. Docherty, M. Edmondson, *J. Phys. Chem. B* **1997**, *101*, 6532.
[44] R. E. Dinnebier, P. W. Stephens, J. K. Carter, A. N. Lommen, P. A. Heiney, A. R. McGhie, L. Brard, A. B. Smith III, *J. Appl. Crystallogr.* **1995**, *28*, 327.
[45] V. V. Chernyshev, H. Schenk, *Z. Kristallogr.* **1998**, *213*, 1.
[46] B. M. Kariuki, H. Serrano-González, R. L. Johnston, K. D. M. Harris, *Chem. Phys. Lett.* **1997**, *280*, 189.
[47] K. Shankland, W. I. F. David, T. Csoka, *Z. Kristall.* **1997**, *212*, 550.
[48] K. D. M. Harris, R. L. Johnston, B. M. Kariuki, M. Tremayne, *J. Chem. Res.* **1998**, 390.
[49] K. D. M. Harris, R. L. Johnston, B. M. Kariuki, *Acta Crystallogr. Sect. A* **1998**, *54*, 632.
[50] *Applications of Synchrotron Radiation* (Eds.: C. R. A. Catlow, G. N. Greaves), Blackie, Glasgow, **1990**.
[51] S. J. Maginn, *Analyst* **1998**, *123*, 19R.
[52] C. C. Wilson, *Acta Crystallogr. Sect. A* **1989**, *45*, 833.
[53] O. J. Lanning, S. Habershon, K. D. M. Harris, R. L. Johnston, B. M. Kariuki, E. Tedesco, G. W. Turner, *Chem. Phys. Lett.* **2000**, *317*, 297.
[54] M. Tremayne, E. J. MacLean, C. C. Tang, C. Glidewell, *Acta Crystallogr. Sect. B* **1999**, *55*, 1068.
[55] P. Lightfoot, M. Tremayne, C. Glidewell, K. D. M. Harris, P. G. Bruce, *J. Chem. Soc. Perkin Trans 2* **1993**, 1625.
[56] J. Cirujeda, L. E. Ochando, J. M. Amigo, C. Rovira, J. Rius, J. Veciana, *Angew. Chem.* **1995**, *107*, 99; *Angew. Chem. Int. Ed. Engl.* **1995**, *34*, 55.
[57] B. M. Kariuki, P. Calcagno, K. D. M. Harris, D. Philp, R. L. Johnston, *Angew. Chem.* **1999**, *111*, 860; *Angew. Chem. Int. Ed.* **1999**, *38*, 831.
[58] P. Calcagno, B. M. Kariuki, S. J. Kitchin, J. M. A. Robinson, D. Philp, K. D. M. Harris, *Chem. Eur. J.* **2000**, *6*, 2338.
[59] P. Calcagno, E. Tedesco, B. M. Kariuki, K. D. M. Harris, D. Philp, unpublished results.
[60] M. Tremayne, C. Glidewell, *Chem. Commun.* **2000**, 2425.
[61] A. M. T. Bell, J. N. B. Smith, J. P. Attfield, J. M. Rawson, K. Shankland, W. I. F. David, *New J. Chem.* **1999**, *23*, 565.
[62] J. D. Dunitz, *Pure Appl. Chem.* **1991**, *63*, 177.
[63] M. R. Caira, *Top. Curr. Chem.* **1998**, *198*, 164.
[64] J. Bernstein, R. J. Davey, J.-O. Henck, *Angew. Chem.* **1999**, *111*, 3646; *Angew. Chem. Int. Ed.* **1999**, *38*, 3440.
[65] R. J. Cernik, A. K. Cheetham, C. K. Prout, D. J. Watkin, A. P. Wilkinson, B. T. M. Willis, *J. Appl. Crystallogr.* **1991**, *24*, 222.
[66] K. Shankland, W. I. F. David, D. S. Sivia, *J. Mater. Chem.* **1997**, *7*, 569.
[67] F. C. Chan, J. Anwar, R. Cernik, P. Barnes, R. M. Wilson, *J. Appl. Crystallogr.* **1999**, *32*, 436.
[68] D. Louër, M. Louër, V. A. Dzyabchenko, V. Agafonov, R. Ceolin, *Acta Crystallogr. Sect. B* **1995**, *51*, 182.
[69] M. Tremayne, W. Dong, C. J. Gilmore, unpublished results.
[70] N. Shankland, A. J. Florence, P. J. Cox, C. C. Wilson, K. Shankland, *Int. J. Pharm.* **1998**, *165*, 107.
[71] K. Shankland, W. I. F. David, T. Csoka, L. McBride, *Int. J. Pharm.* **1998**, *165*, 117.
[72] B. M. Kariuki, K. Psallidas, K. D. M. Harris, R. L. Johnston, R. W. Lancaster, S. E. Staniforth, S. M. Cooper, *Chem. Commun.* **1999**, 1677.
[73] P. Lightfoot, M. Tremayne, K. D. M. Harris, P. G. Bruce, *J. Chem. Soc. Chem. Commun.* **1992**, 1012.
[74] K. D. Knudsen, P. Pattison, A. N. Fitch, R. J. Cernik, *Angew. Chem.* **1998**, *110*, 2474; *Angew. Chem Int. Ed.* **1998**, *37*, 2340.
[75] M. Tremayne, B. M. Kariuki, K. D. M. Harris, *J. Mater. Chem.* **1996**, *6*, 1601.
[76] B. M. Kariuki, D. M. S. Zin, M. Tremayne, K. D. M. Harris, *Chem. Mater.* **1996**, *8*, 565.
[77] J. A. Kaduk, J. T. Golab, *Acta Crystallogr. Sect. B* **1999**, *55*, 85.
[78] D. Seebach, J. L. Matthews, A. Meden, T. Wessels, C. Baerlocher, L. B. McCusker, *Helv. Chim. Acta* **1997**, *80*, 173.
[79] V. V. Chernyshev, A. V. Yatsenko, V. A. Tafeenko, S. G. Zhukov, L. A. Aslanov, E. J. Sonneveld, H. Schenk, V. A. Makarov, V. G. Granik, V. A. Trounov, A. I. Kurbakov, *Z. Kristallogr.* **1998**, *213*, 477.
[80] H. R. Karfunkel, Z. J. Wu, A. Burkhard, G. Rihs, D. Sinnreich, H. M. Buerger, J. Stanek, *Acta Crystallogr. Sect. B* **1996**, *52*, 555.
[81] A. N. Fitch, H. Jobic, *J. Chem. Soc. Chem. Commun.* **1993**, 1516.
[82] J. Min, J. Benet-Buchholz, R. Boese, *Chem. Commun.* **1998**, 2751.
[83] A. J. Mora, A. N. Fitch, *J. Solid State Chem.* **1997**, *134*, 211.
[84] E. Tedesco, G. W. Turner, K. D. M. Harris, R. L. Johnston, B. M. Kariuki, *Angew. Chem.* **2000**, *112*, 4662; *Angew. Chem. Int. Ed.* **2000**, *39*, 4488.
[85] G. W. Turner, E. Tedesco, K. D. M. Harris, R. L. Johnston, B. M. Kariuki, *Chem. Phys. Lett.* **2000**, *321*, 183.
[86] G. Fischer, *Chem. Soc. Rev.* **2000**, *29*, 119.
[87] L. E. Ochando, J. Rius, D. Louër, R. M. Claramunt, C. Lopez, J. Elguero, J. M. Amigo, *Acta Crystallogr. Sect. B* **1997**, *53*, 939.
[88] N. Masciocchi, A. Sironi, *J. Chem. Soc. Dalton Trans.* **1997**, 4643.
[89] R. E. Dinnebier, F. Olbrich, S. van Smaalen, P. W. Stephens, *Acta Crystallogr. Sect. B* **1997**, *53*, 153.
[90] A. Altomare, G. Cascarano, C. Giacovazzo, A. Guagliardi, M. C. Burla, G. Polidori, M. Camalli, *J. Appl. Crystallogr.* **1994**, *27*, 435.
[91] P. Miao, A. W. Robinson, R. E. Palmer, B. M. Kariuki, K. D. M. Harris, *J. Phys. Chem.* **2000**, *104*, 1285.
[92] S. Pagola, P. W. Stephens, D. S. Bohle, A. D. Kosar, S. K. Madsen, *Nature* **2000**, *404*, 307.
[93] J. M. Thomas, *Angew. Chem.* **1988**, *100*, 1735; *Angew. Chem. Int. Ed. Engl.* **1988**, *27*, 1673.
[94] J. M. Thomas, *Angew. Chem.* **1994**, *106*, 963; *Angew. Chem. Int. Ed. Engl.* **1994**, *33*, 913.
[95] J. M. Thomas, *Angew. Chem.* **1999**, *111*, 3800; *Angew. Chem. Int. Ed.* **1999**, *38*, 3588.
[96] J. M. Thomas, D. E. W. Vaughan, *J. Phys. Chem. Solids* **1989**, *50*, 449.

[97] Z. A. Kaszkur, R. H. Jones, D. Waller, C. R. A. Catlow, J. M. Thomas, *J. Phys. Chem.* **1993**, *97*, 426.
[98] L. B. McCusker, *Stud. Surf. Sci. Catal.* **1994**, *84*, 341.
[99] W. M. Meier, D. H. Olson, C. Baerlocher, *Atlas of Zeolite Structure Types*, 4. Aufl., Elsevier, New York, **1996**.
[100] P. R. Rudolf, C. Saldarriaga-Molina, A. Clearfield, *J. Phys. Chem.* **1986**, *90*, 6122.
[101] L. B. McCusker, *J. Appl. Crystallogr.* **1988**, *21*, 305.
[102] D. M. Poojary, J. O. Perez, A. Clearfield, *J. Phys. Chem.* **1992**, *96*, 7709.
[103] P. A. Barrett, M. A. Camblor, A. Corma, R. H. Jones, L. A. Villaecusa, *Chem. Mater.* **1997**, *9*, 1713.
[104] H. Gies, J. Rius, *Z. Kristallogr.* **1995**, 210, 475.
[105] A. Simmen, L. B. McCusker, C. Baerlocher, W. M. Meier, *Zeolites* **1991**, *11*, 654.
[106] S. Brenner, L. B. McCusker, C. Baerlocher, *J. Appl. Crystallogr.* **1997**, *30*, 1167.
[107] R. W. Grosse-Kunstleve, L. B. McCusker, C. Baerlocher, *J. Appl. Crystallogr.* **1997**, *30*, 985.
[108] H. Gies, B. Marler, S. Vortmann, U. Oberhagemann, P. Bayat, K. Krink, J. Rius, I. Wolf, C. Fyfe, *Microporous Mesoporous Mater.* **1998**, *21*, 183.
[109] R. W. Grosse-Kunstleve, L. B. McCusker, C. Baerlocher, *J. Appl. Crystallogr.* **1999**, *32*, 536.
[110] R. W. Grosse-Kunstleve, Dissertation, Nr. 11422, ETH Zürich, **1996**.
[111] M. W. Deem, J. M. Newsam, *Nature* **1989**, *342*, 260.
[112] M. W. Deem, J. M. Newsam, *J. Am. Chem. Soc.* **1992**, *114*, 7189.
[113] D. E. Akporiye, H. Fjellvag, E. N. Halvorsen, J. Hustveit, A. Karlsson, K. P. Lillerud, *J. Phys. Chem.* **1996**, *100*, 16641.
[114] B. J. Campbell, G. Bellussi, L. Carluccio, G. Perego, A. K. Cheetham, D. E. Cox, R. Millini, *Chem. Commun.* **1998**, 1725.
[115] T. Wessels, C. Baerlocher, L. B. McCusker, *Science* **1999**, *284*, 477.
[116] S. Hanna, P. D. Coulter, A. H. Windle, *J. Chem. Soc. Faraday Trans.* **1995**, *91*, 2615.
[117] R. J. Pazur, P. J. Hocking, S. Raymond, R. H. Marchessault, *Macromolecules* **1998**, *31*, 6585.
[118] S. Bruckner, S. Destri, W. Porzio, *Macromol. Rapid. Commun.* **1995**, *16*, 297.
[119] N. Masciocchi, M. Moret, P. Cairati, A. Sironi, G. A. Ardizzoia, G. La Monica, *J. Am. Chem. Soc.* **1994**, *116*, 7668.
[120] N. Masciocchi, M. Moret, P. Cairati, A. Sironi, G. A. Ardizzoia, G. La Monica, *J. Chem. Soc. Dalton Trans.* **1995**, 1671.
[121] N. Masciocchi, P. Cairati, L. Carlucci, G. Ciani, G. Mezza, A. Sironi, *J. Chem. Soc. Dalton Trans.* **1994**, 3009.
[122] N. Masciocchi, P. Cairati, L. Carlucci, G. Meeza, G. Ciani, A. Sironi, *J. Chem. Soc. Dalton Trans.* **1996**, 2739.
[123] N. Masciocchi, R. Bianchi, P. Cairati, G. Mezza, T. Pilati, A. Sironi, *J. Appl. Crystallogr.* **1994**, *27*, 426.
[124] N. Masciocchi, G. A. Ardizzoia, G. La Monica, A. Maspero, A. Sironi, *Angew. Chem.* **1998**, *110*, 3561; *Angew. Chem. Int. Ed.* **1998**, *37*, 3366.
[125] P. Lightfoot, M. A. Mehta, P. G. Bruce, *J. Mater. Chem.* **1992**, *2*, 379.
[126] P. Lightfoot, M. A. Mehta, P. G. Bruce, *Science* **1993**, *262*, 883.
[127] P. Lightfoot, J. L. Nowinski, P. G. Bruce, *J. Am. Chem. Soc.* **1994**, *116*, 7469.
[128] J. B. Thomson, P. Lightfoot, P. G. Bruce, *Solid State Ionics* **1996**, *85*, 203.
[129] Y. G. Andreev, G. S. MacGlashan, P. G. Bruce, *Phys. Rev. B* **1997**, *55*, 12011.
[130] G. S. MacGlashan, Y. G. Andreev, P. G. Bruce, *Nature* **1999**, *398*, 792.
[131] H. Zollinger, *Color Chemistry*, 2. Aufl, VCH, Weinheim, **1991**.
[132] P. G. Fagan, R. B. Hammond, K. J. Roberts, R. Docherty, A. P. Chorlton, W. Jones, G. D. Potts, *Chem. Mater.* **1995**, *7*, 2322.
[133] A. V. Yatsenko, V. V. Chernyshev, L. A. Aslanov, H. Schenk, *Powder Diffr.* **1998**, *13*, 85.
[134] R. B. Hammond, K. J. Roberts, R. Docherty, M. Edmondson, R. Gairns, *J. Chem. Soc. Perkin Trans. 2* **1996**, 1527.
[135] M. U. Schmidt, R. E. Dinnebier, *J. Appl. Crystallogr.* **1999**, *32*, 178.
[136] J. S. Zambounis, Z. Hao, A. Iqbal, *Nature* **1997**, 388, 131.
[137] E. J. MacLean, PhD Thesis, University of London, **1997**.
[138] E. J. MacLean, M. Tremayne, B. M. Kariuki, K. D. M. Harris, A. F. M. Iqbal, Z. Hao, *J. Chem. Soc. Perkin Trans. 2* **2000**, 1513.
[139] M. D. Cohen, G. M. J. Schmidt, F. I. Sonntag, *J. Chem. Soc.* **1964**, 2000.
[140] G. M. J. Schmidt, *Pure Appl. Chem.* **1971**, *27*, 647.
[141] J. M. Thomas, *Philos. Trans. R. Soc. London A* **1974**, *277*, 251.
[142] R. Hoffmann, *Liebigs Ann. Chem.* **1857**, *102*, 1.
[143] A. Kekulé, *Liebigs Ann. Chem.* **1858**, *105*, 288.
[144] L. Elizabé, B. M. Kariuki, K. D. M. Harris, M. Tremayne, M. Epple, J. M. Thomas, *J. Phys. Chem. B* **1997**, *101*, 8827.
[145] H. Ehrenberg, B. Hasse, K. Schwarz, M. Epple, *Acta Crystallogr. Sect. B* **1999**, *55*, 517.
[146] R. E. Dinnebier, R. Von Dreele, P. W. Stephens, S. Jelonek, J. Sieler, *J. Appl. Crystallogr.* **1999**, *32*, 761.
[147] J. Hulliger, *Angew. Chem.* **1994**, *106*, 151; *Angew. Chem. Int. Ed. Engl.* **1994**, *33*, 143.
[148] K. D. M. Harris, I. L. J. Patterson, *J. Chem. Soc. Perkin Trans. 2* **1994**, 1201.
[149] H. Nakanishi, M. Hasegawa, T. Mori, *Acta Crystallogr. Sect. C* **1985**, *41*, 70.
[150] N. Masciocchi, M. Bergamo, A. Sironi, *Chem. Commun.* **1998**, 1347.
[151] G. B. Hix, D. S. Wragg, P. A. Wright, R. E. Morris, *J. Chem. Soc. Dalton Trans.* **1998**, 3359.
[152] D. Braga, L. Maini, F. Grepioni, *Chem. Commun.* **1999**, 937.
[153] J. W. Visser, *J. Appl. Crystallogr.* **1969**, *2*, 89.
[154] P.-E. Werner, L. Eriksson, M. Westdahl, *J. Appl. Crystallogr.* **1985**, *18*, 367.
[155] A. Boultif, D. Louër, *J. Appl. Crystallogr.* **1991**, *24*, 987.
[156] R. A. Shirley, *CRYSFIRE* Suite of Programs for Indexing Powder Diffraction Patterns, University of Surrey.
[157] J. I. Langford, D. Louër, D. *Rep. Progr. Phys.* **1996**, *59*, 131.
[158] "Data Accuracy for Powder Indexing": R. Shirley, *NBS Spec. Publ. (U.S.)* **1980**, *567361*.
[159] "Accuracy in Powder Diffraction II": D. Louër, *NIST Spec. Publ.* **1992**, *846*, 92 – 104.
[160] B. M. Kariuki, S. A. Belmonte, M. I. McMahon, R. L. Johnston, K. D. M. Harris, R. J. Nelmes, *J. Synchrotron Radiat.* **1999**, *6*, 87.
[161] W. Paszkowicz, *Mater. Sci. Forum* **1996**, *228 – 231*, 19.
[162] R. A. Young, D. B. Wiles, *J. Appl. Crystallogr.* **1982**, *15*, 430.
[163] R. E. Dinnebier, M. Pink, J. Sieler, P. W. Stephens, *Inorg. Chem.* **1997**, *36*, 3398.
[164] R. E. Dinnebier, M. Pink, J. Sieler, P. Norby, P. W. Stephens, *Inorg. Chem.* **1998**, *37*, 4996.
[165] N. Metropolis, A. W. Rosenbluth, M. N. Rosenbluth, A. H. Teller, E. Teller, *J. Chem. Phys.* **1953**, *21*, 1087.
[166] M. P. Allen, D. J. Tildesley, *Computer Simulation of Liquids*, Oxford University Press, Oxford, **1987**.
[167] P. J. M. van Laarhoven, E. H. L. Aarts, *Simulated Annealing: Theory and Applications*, D. Riedel Publishing, Holland, **1987**.
[168] J. Holland, *Adaptation in Natural and Artificial Systems*, University of Michigan Press, Ann Arbor, MI, **1975**.
[169] D. E. Goldberg, *Genetic Algorithms in Search, Optimization and Machine Learning*, Addison-Wesley, Reading, Massachusetts, **1989**.
[170] H. M. Cartwright, *Applications of Artificial Intelligence in Chemistry*, Oxford University Press, Oxford, **1993**.
[171] K. D. M. Harris, R. L. Johnston, B. M. Kariuki, *An. Quim. Int. Ed.* **1998**, *94*, 410.
[172] B. M. Kariuki, R. L. Johnston, K. D. M. Harris, K. Psallidas, S. Ahn, H. Serrano-González, *Comm. Math. Comp. Chem.* **1998**, *38*, 123.
[173] T. Csoka, W. I. F. David, K. Shankland, *Mater. Sci. Forum* **1998**, *278 – 281*, 294.
[174] E. Tedesco, G. W. Turner, K. D. M. Harris, R. L. Johnston, B. M. Kariuki, unpublished results.
[175] C. J. Gilmore, K. Henderson, G. Bricogne, *Acta Crystallogr. Sect. A* **1991**, *47*, 830.
[176] A. C. Larson, R. B. Von Dreele, *Los Alamos Natl. Lab. Rep.* **1987**, LA-UR-86-748.
[177] J. Rodriguez-Carvajal in *Collected Abstracts of Powder Diffraction Meeting*, Toulouse, France, **1990**, p. 127.
[178] J. K. Cockcroft, *PROFIL*, Version 5.17, Department of Crystallography, Birkbeck College, UK, **1994**.
[179] D. B. Wiles, R. A. Young, *J. Appl. Crystallogr.* **1981**, *14*, 149.
[180] F. Izumi, H. Asano, H. Murata, N. Watanabe, *J. Appl. Crystallogr.* **1987**, *20*, 411.

[181] W. A. Dollase, *J. Appl. Crystallogr.* **1986**, *19*, 267.
[182] A. Altomare, G. Cascarano, C. Giacovazzo, A. Guagliardi, *J. Appl. Crystallogr.* **1994**, *27*, 1045.
[183] R. Peschar, H. Schenk, P. Capkov, *J. Appl. Crystallogr.* **1995**, *28*, 127.
[184] M. Tremayne, B. M. Kariuki, K. D. M. Harris, unpublished results.
[185] C. B. Aakeroy, A. M. Beatty, D. M. Rowe, C. C. Seaton, M. Tremayne, unpublished results.
[186] R. B. Von Dreele, *J. Appl. Crystallogr.* **1999**, *32*, 1084.
[187] J. M. Robertson, *Organic Crystals and Molecules*, Cornell University Press, Ithaca, New York, **1953**.